https://doi.org/10.5194/acp-2021-132
Preprint. Discussion started: 23 March 2021

Atmospheric Chemistry and Physics Discussions

On the competing effects of contemporary land management vs. land cover changes on global air quality

Anthony Y. H. Wong, Jeffrey A. Geddes
Department of Earth and Environment, Boston University, Boston, MA, USA

Correspondence to: Jeffrey A. Geddes (jgeddes@bu.edu)

Abstract. Our work explores the impact of two important dimensions of land system changes, land use and land cover change (LULCC) and direct agricultural reactive nitrogen (N_r) emissions from soils, on ozone (O_3) and fine particulate matter ($PM_{2.5}$) air quality over contemporary (1992 to 2014) time scales. We account for LULCC and agricultural N_r emissions changes with consistent remote sensing products and new global emission inventories, respectively, estimating their impacts on global surface O_3 and $PM_{2.5}$ concentrations and N_r deposition using the GEOS-Chem global chemical transport model. Over this time period, our model results show that agricultural N_r emission changes cause reduction of annual mean $PM_{2.5}$ level over Europe and northern Asia (up to -2.1 μg m^{-3}), while increasing $PM_{2.5}$ level India, China and eastern US (up to +3.5 μg m^{-3}). Land cover changes induce small reductions in $PM_{2.5}$ (up to -0.7 μg m^{-3}) over Amazonia, China and India due to reduced biogenic volatile organic compounds (BVOC) emissions and enhanced deposition of aerosol precursor gases (e.g. NO_2, SO_2). Agricultural N_r emission changes only lead to minor changes (up to ± 0.6 ppbv) in annual mean surface O_3 level, mainly over China, India and Myanmar. Meanwhile, our model result suggests a stronger impact of LULCC on surface O_3 over the time period Across South America, the combination of changes in dry deposition and isoprene emissions results in -0.8 to +1.2 ppbv surface ozone changes. The enhancement of dry deposition reduces surface ozone level (up to -1 ppbv) over southern China, eastern US and central Africa. The enhancement of soil NOx emission due to crop expansion also contribute to surface ozone changes (up to +0.6 ppbv) over sub-Saharan Africa. In certain regions, the combined effects of LULCC and agricultural N_r emission changes on O_3 and $PM_{2.5}$ air quality can be comparable (> 20%) to that of anthropogenic emission changes over the same time period. Finally, we calculate that the increase in global agricultural N_r emissions leads to a net increase in global land area (+3.67 ×10^6 km^2) that potentially faces exceedance in critical N_r load (> 5 kgN ha^{-1} yr^{-1}). Our result demonstrates the possible impacts of contemporary LULCC and agricultural N_r emission changes on $PM_{2.5}$ and O_3 air quality, which also implies the potential importance of land system changes on air quality over multi-decadal timescales.

1 Introduction

The broad term of land use and land cover change (LULCC) encapsulates both the anthropogenic (e.g. agricultural expansion) and natural (e.g. ecological succession) dimensions of terrestrial biome changes (Reick et al., 2013), which alter the physical and ecophysiological properties of the land surface. These perturbations alter the transfer and uptake of air pollutants by ecosystems, and can also have large impacts on the emission of biogenic volatile organic compounds (BVOCs), which play

https://doi.org/10.5194/acp-2021-132
Preprint. Discussion started: 23 March 2021

Atmospheric Chemistry and Physics Discussions

vital roles in tropospheric ozone (O_3) and secondary organic aerosol (SOA) formation (Fu and Tai, 2015; Ganzeveld et al., 2010; Heald and Geddes, 2016; Heald and Spracklen, 2015; Squire et al., 2014; Wu et al., 2012a).

Agricultural activities, in addition to being a large driver of LULCC (e.g. Ellis, 2015; Ellis et al., 2013; Goldewijk et al., 2017; Kaplan et al., 2011), also introduce enormous amount of reactive nitrogen into the soil (Galloway et al., 2008), which can be emitted into the atmosphere either as oxidized or reduced nitrogen. NO_x (≡ NO + NO_2) is a key component of O_3 photochemistry. Reactive nitrogen also contributes to aerosol formation (Ansari and Pandis, 1998). Indeed, agricultural emissions are the dominant global anthropogenic source of ammonia (NH_3) (Hoesly et al., 2018), and identified as a major contributor to global premature mortality due to particulate matter (PM) pollution (Lelieveld et al., 2015). Trends in atmospheric reactive nitrogen also affect nitrogen deposition (e.g. Geddes and Martin, 2017), with potentially negatively impacts on biodiversity (e.g. Bobbink et al., 2010; Payne et al., 2017; WallisDeVries and Bobbink, 2017), or eutrophication of aquatic ecosystems (e.g. Fenn et al., 2003). These ecosystem impacts may contribute to economic loss comparable to the benefits of extra crop output from LULCC and agricultural emissions (Paulot and Jacob, 2014; Sobota et al., 2015).

Even while land cover at a particular location may not change, modifications in human management of the land (e.g. intensification of agriculture, irrigation practices, fertilizer application, selective harvesting) may still be associated with changes in pollutant emission and uptake. An obvious example would be a region where direct agricultural emissions may have changed, without any concomitant changes in land cover classification. Reducing NH_3 emission, particularly from the agricultural sector, has been explored as a potent strategy of controlling PM pollution (Giannadaki et al., 2018; Pinder et al., 2007; Pozzer et al., 2017). Bauer et al. (2016) suggest agricultural emissions are the main source of present-day $PM_{2.5}$ (fine particulates with an aerodynamic diameter less than 2.5 μm) over eastern US, Europe and northern China. However, as anthropogenic NO_x and SO_2 emissions are expected to lower in the future, some aerosol formation chemistry is expected to become less sensitive to NH_3 emissions.

The potential impacts of LULCC and agricultural emission changes on air quality have been explored previously. To date, this work has focused on future projections in land use (Bauer et al., 2016; Ganzeveld et al., 2010; Hardacre et al., 2013; Heald et al., 2008; Squire et al., 2014; Tai et al., 2013; Wu et al., 2012b), contrasted pre-industrial estimates of land cover and agricultural emissions with present-day conditions (Heald and Geddes, 2016; Hollaway et al., 2017), or are regional in focus (Fu and Tai, 2015; Geddes et al., 2015; Silva et al., 2016). For example, Wu et al. (2012) propose that LULCC induced by climate, CO_2 abundance, and agriculture could significantly affect surface O_3 in the future mainly through modulating dry deposition and isoprene emissions. Over more contemporary timescales (e.g. across the last 20-30 years), Fu et al. (2016), Fu and Tai (2015) and Silva et al., (2016) find that LULCC could have impacts O_3 and PM air quality over China and Southeast Asia.

https://doi.org/10.5194/acp-2021-132
Preprint. Discussion started: 23 March 2021


Atmospheric Chemistry and Physics Discussions

Given the large spatial scale of LULCC (e.g. Hansen et al., 2013; Li et al., 2018) and agricultural emission changes (e.g. Crippa et al., 2018; Hoesly et al., 2018; Xu et al., 2019) over recent decades, these two land system changes could be contributing substantially to global trends in O_3 and PM pollution. While changes in land cover and agricultural emissions actually occur contemporaneously across the globe, they are rarely considered together in simulations of air quality from chemical transport models. As a result, it is not clear to what extent LULCC may either amplify or offset the impacts of some of the associated agricultural emission changes, how this may vary regionally, and to what extent these land system impacts may compare to concomitant changes resulting from other direct anthropogenic emissions (e.g. emissions from industrial and transport sectors).

The recent availability both of consistent long-term land records of land cover derived from satellite remote sensing observations, and global anthropogenic emission inventories, opens an opportunity for a more holistic and observationally-constrained assessment of the impacts on global O_3 and PM air quality from contemporary changes in LULCC and agricultural emissions simultaneously, and a comparison of these with the effects from direct anthropogenic emissions. In this study, we model the effects of contemporary LULCC and agriculture emissions changes on global surface O_3 and $PM_{2.5}$ levels, and gauge their importance relative to changes in other direct anthropogenic emissions over the same period of time. We also highlight the effect of agricultural emissions changes on nitrogen deposition on land ecosystems. Through our chemical transport model predictions, we aim to identify potential global hotspots of contemporary land changes that may be substantially altering trends in air quality and nitrogen deposition.

2 Method

To simulate global changes in surface O_3 and $PM_{2.5}$ concentrations due to LULCC, agricultural emissions, and direct anthropogenic emissions over 1992 to 2014, we use the GEOS-Chem chemical transport model (version 12.7.0, https://doi.org/10.5281/zenodo.3634864). We choose our timeframe due to the availability of consistent high-resolution remote sensing products (PFT and LAI maps) and concurrent global emission inventories. We define "direct anthropogenic" and "agricultural" emissions separately in more detail below.

We perform five sets of simulations summarized in Table 1: (1) a "baseline" scenario where land cover, agricultural emissions, and direct anthropogenic emissions are all set to 1992 levels; (2) an "anthropogenic emission" scenario where direct anthropogenic emissions are updated to 2014 levels; (3) a "anthropogenic emissions and land cover change" scenario where anthropogenic emissions remain updated to 2014, with land cover inputs now prescribed based on updated 2014 data; and (4) an "anthropogenic emissions, land cover, and agricultural emission change" scenario where direct anthropogenic emissions and land cover inputs remain updated to 2014, with agricultural emissions also updated to 2014 levels. To test the chemical sensitivity of our results, a fifth scenario is performed where anthropogenic emissions are held at 1992 levels, but land cover change and agricultural emissions are updated to 2014 levels.

https://doi.org/10.5194/acp-2021-132
Preprint. Discussion started: 23 March 2021


Atmospheric Chemistry and Physics Discussions

The role of direct anthropogenic emission changes can be evaluated by comparing simulation (1) and (2); the additional role played by land cover changes over this time period is evaluated by comparing simulation (2) and (3); and finally the additional impact of agricultural emission changes is evaluated by comparing simulation (3) and (4). The latter two effects will be the focus of this paper, but we compare these to the role of direct anthropogenic emission changes for context. Since changes in surface ozone and $PM_{2.5}$ should be sensitive to NO_x-VOC ratio and availability of NO_3^- and SO_4^{2-} ions, the sensitivity of the effects from land cover change and agricultural emission changes to anthropogenic emission changes can be quantified by evaluating simulation (5).

We use assimilated meteorological fields from Modern-Era Retrospective analysis for Research and Applications Version 2 (MERRA-2) (Gelaro et al., 2017) to drive GEOS-Chem. All simulations are carried out at 2° latitudes by 2.5° longitudes resolution over the globe, using identical meteorological fields from 2011 to 2014 in order to exclude meteorological variability from the analysis. The output from 2011 is discarded as spin-up. The GEOS-Chem model simulates O_3 chemistry with a comprehensive HO_x-NO_x-VOC-O_3-BrO_x chemical mechanism (Bey et al., 2001; Mao et al., 2013). Gaseous dry deposition follows Wang et al. (1998) and Wesely (1989), while particle deposition follows Zhang et al. (2001). Wet deposition is described by Liu et al. (2001) with updates from Amos et al. (2012) and Wang et al. (2011, 2014). The recent update from Luo et al., (2019) on wet deposition parameterization is also included to improve model-observation agreement for sulfate-nitrate-ammonium (SNA) aerosol. The thermodynamics and gas-aerosol partitioning of the NH_3-H_2SO_4-HNO_3 system is simulated by ISORROPIA II module (Fountoukis and Nenes, 2007). A simple yield-based secondary organic aerosol (SOA) estimate is also included (Kim et al., 2015). Other types of aerosol represented in the model include sea salt, dust, primary black carbon (BC) and organic carbon (OC). The total $PM_{2.5}$ mass is then calculated at 35% relative humidity for consistency with the measurement standard in US.

We use anthropogenic and agricultural emissions based on the Community Emission Data System (CEDS) inventory (Hoesly et al., 2018), which contains the estimates of anthropogenic NO_x, non-methane volatile organic compounds (NMVOCs), CO, BC, OC, SO_2 and NH_3 harmonized from a wide range of global and regional inventories. In this inventory, emissions are from six major sectors: energy production, industry, transportation, RCO (residential, commercial, other), agriculture, and waste. For this study, "agricultural emissions" specifically refer to NO_x and NH_3 emitted from fertilizer application and manure management, which correspond directly to agricultural nitrogen input. We do not consider the changes in agricultural of other trace species (e.g. CH_4, SO_2, CO).

Biogenic volatile organic compound emissions are calculated by Model of Emissions of Gases and Aerosols from Nature (MEGAN) v2.1 (Guenther et al., 2012). Soil NO_x emission follows Hudman et al. (2012), with fertilizer emissions zeroed out to avoid double counting with the agricultural NO_x emission in CEDS inventory. Fire (Global Fire Emissions Database v4.1, Van Der Werf et al., 2017) and lightning (Murray et al., 2012) emissions are held constant at 2014 level.

https://doi.org/10.5194/acp-2021-132
Preprint. Discussion started: 23 March 2021


Atmospheric Chemistry and Physics Discussions

We use the European Space Agency Climate Change Initiative (ESA CCI) land cover map (Li et al., 2018) to characterize LULCC and drive the biosphere-atmosphere emission fluxes in our simulations. The ESA CCI land cover map is a consistent global annual land cover time series derived from the satellite observations from the AVHRR, MERIS, SOPTVGT and PROBA-V instruments. It has a native spatial resolution of 300 m following the United Nations Land Cover Classification System. Time-consistent land surface characterization also requires leaf area index (LAI) data. We use the Global Land Surface Satellite (GLASS) product (Xiao et al., 2016) (retrieved from http://globalchange.bnu.edu.cn/), which is a global LAI time series combining AVHRR and MODIS observation. 3-year average (1991 – 1993 average LAI for 1992 land cover, 2013 – 2015 average LAI for 2014 land cover) is used as input for LAI to GEOS-Chem to reduce the possible effect of interannual variability.

This satellite-derived land surface characterization on its own is not directly compatible with the input to the vegetation-related modules in GEOS-Chem, thus requires further harmonization (dry deposition, BVOC emissions, soil NO_x emissions), which is a common problem for simulations involving land change (e.g. Geddes et al., 2016). We first aggregate and process the ESACCI land cover map with the tool and crosswalk table provided with the land cover product to derive the percentage coverage of plant functional type (PFT) at 0.05° resolution, which is the native resolution of GLASS LAI. The dominant surface type can be readily mapped to the 11 deposition surface type in the Wesely dry deposition model. We adopt the approach of Geddes et al. (2016) to replace roughness length (z_0) from assimilated meteorology with that prescribed for each deposition surface type. To derive the MODIS-Koeppen type land map (Steinkamp and Lawrence, 2011) required for soil NO_x module, we first use translate the PFT map according to International Geosphere-Biosphere Programme (IGBP) land cover classification system (http://www.eomf.ou.edu/static/IGBP.pdf). We use global monthly temperature climatology (Matsuura and Willmott, 2012) to further differentiate the land types by climate with criteria outlined by Kottek et al. (2006). Finally, the ESA CCI PFT map is converted to Community Land Model (CLM) PFT map, which is required for MEGAN BVOC emissions module, by the temperature criteria specified by Bonan et al. (2002). As the method of deriving C3:C4 grass ratio was subsequently updated (Lawrence and Chase, 2007), this ratio is directly taken from CLM land surface data set.

In the Supplementary Material, we provide an evaluation of the annual mean simulated SNA aerosol mass concentration and surface O_3 mixing ratios from the Simulation 4 (representative of 2014 conditions) with globally available observations from the same time period. In general, the model captures the regional annual means of individual SNA species reasonably (Fig. S1 and Table S1), especially over US and Europe where the bias is within ±30%. The model underestimates all SNA species over China in a relatively uniform fashion (36 – 55%). Over the region covered by Acid Deposition Monitoring Network in East Asia (EANET) (Japan, Korea and southeast Asia) the model underestimates the negatively charge ions (36% for sulphate and 16% for nitrate) while overestimating ammonium by 14%. Figure S2 shows the reasonable agreement on annual mean surface O_3 between our model output and the gridded observation dataset from Sofen et al. (2016) (mean bias = +1.81 ppbv and mean

https://doi.org/10.5194/acp-2021-132
Preprint. Discussion started: 23 March 2021


Atmospheric Chemistry and Physics Discussions

absolute error = 3.97 ppbv). Our model therefore captures the present-day annual means of surface SNA and O_3 concentrations, providing basis for our subsequent analyses.

3 Changes in Land Cover, and Biospheric Fluxes, and Agricultural Emissions

Table 2 shows the changes in global coverage of the major land cover types from 1992 to 2014 derived by the ESA CCI land cover product. The coverage of managed grass (including cropland and pasture) and built-up area, both of which are unmistakably related to human activities, have increased mainly at the expense of forest coverage, indicative of a global trend in deforestation over this period. Figure 1 shows the spatial distribution of changes in fractional coverage of the major land cover types. Expansion of agricultural land at the expense of broadleaf forest coverage is most notable in southern Amazonia and Southeast Asia, which is well-documented in other studies based on remote sensing (Hansen et al., 2013) and national surveys (Keenan et al., 2015). The expansion of agricultural land over this time period is also observed in central Asia, African savannah, southeastern Australia, South China and North Africa, but usually at the expense of land types other than broadleaf forests (mainly primary grassland and needleleaf forests). Meanwhile, transitions from agricultural land to forests and built-up areas is observed in northern China and eastern Europe, consistent with the findings of Potapov et al. (2015) and Lai et al. (2016).

Figure 2 shows the global changes in 3-year (2012-2014 minus 1991-1993) annual mean LAI calculated from the GLASS LAI data set. Over South China, Paraguay and northern Argentina, the area with regionally consistent deforestation experience general increase in LAI, while the opposite effect is observed in African savannah and central Asia. In Europe, LAI decreases in Ukraine, Poland, Germany, but increases in most other parts despite a fairly consistent retraction of agricultural land is observed over the whole Europe. The agricultural expansion and deforestation over Southeast Asia is mostly concurrent with the LAI decreases. LAI increases notably in northern China where agricultural land decreases. The fact that LAI change can be driven by factors other than changes in land cover type (e.g. temperature, precipitation, atmospheric CO_2 level) (e.g. Zhu et al., 2016) may explain the regionally divergent trends response of LAI to agricultural land use change. We note that since the relationship between satellite-derived surface reflectance and retrieved LAI depends on land cover, the use of static land cover map in long-term LAI retrievals (Claverie et al., 2016; Xiao et al., 2016; Zhu et al., 2013) may not fully capture the effect of LULCC on LAI (Fang et al., 2013).

These changes in land cover produce changes in the biogenic fluxes of reactive trace gases between the Earth's surface and atmosphere derived by GEOS-Chem. Figure 3a shows the calculated changes in annual mean isoprene emission due to land cover change over 1992 to 2014, and suggests that global isoprene emission could have decreased by 5.12 Tg/yr (-1.5 %). The largest local reductions in isoprene emissions are observed in southern Amazonia, Paraguay and northern Argentina, where deforestation from highly isoprene-emitting broadleaf forests is most strongly observed, causing decreases in isoprene

https://doi.org/10.5194/acp-2021-132
Preprint. Discussion started: 23 March 2021


Atmospheric Chemistry and Physics Discussions

emissions by up to 30%. We note that the decrease of isoprene emission simulated in Southeast Asia does not agree with the result from Silva et al. (2016), since our remote sensing data does not have separate land cover class for oil palm plantations which have expanded dramatically in the region. Our model may not therefore capture the full effects of LULCC on isoprene emission, and its effect on $PM_{2.5}$ and O_3 over the region. Elsewhere in the world, the signals of land cover change on isoprene emissions are mostly small and follow the local patterns of changes in LAI. Changes in monoterpenes (< 5 ng m^{-2} s^{-1}) and sesquiterpene (< 1 ng m^{-2} s^{-1}) emissions are relatively small.

Figure 3b shows the changes in annual mean soil NO emission due to LULCC, which represent the change in soil emission driven purely by LAI and land cover changes (i.e. without considering the changes in nitrogen input). LULCC leads to a small signal of +0.04 TgN/yr (+0.6%) in global soil NO emission. The magnitude of changes in soil NO emission induced by LULCC is comparable to that in agricultural NO emissions inventory (see below) over certain regions (e.g. South America, Australia, Sub-Saharan Africa). Relatively large increases in soil NO is simulated over western Africa.

Figure 3c shows the changes in annual mean O_3 dry deposition velocity (v_d), which also closely follow the pattern of LAI changes. Slight increases of v_d are observed in China, India, Southeast US, Mexico, northern Amazonia, Europe and southern Africa (SAf). In Southeast Asia v_d decreases concurrently with deforestation and reduction in LAI. In central Brazil, the increase in LAI is offset by the deforestation of tropical evergreen broadleaf forests that have higher v_d than other land types (Song-Miao Fan et al., 1990; Wang et al., 1998), leading to small overall change in v_d. Likewise, despite deforestation observed in the savannah and grassland over Rio de la Plata basin, these losses are offset by strong increases in LAI so that v_d increases by up to 0.1 cm s^{-1}. Significant changes in the v_d of O_3 due to LAI also imply that v_d of other relevant trace gases (e.g. NO_2, SO_2) would also be perturbed by land cover change in our model, which will be discussed briefly in the subsequent section.

Figure 4 shows the changes in agricultural NH_3 and NO_x emissions between 1992 and 2014, which consists mostly of emissions from fertilizer application and manure management (Hoesly et al., 2018). According to the CEDS inventory, global direct agricultural NH_3 emissions increased by 7.6 Tg N/yr since 1992, equivalent to a 19 % increase in total anthropogenic NH_3 emissions. Direct agricultural soil NOx emissions increased by 0.37 Tg N/yr since 1992, and while this is a substantial increase in agricultural soil NOx emissions (26 %), it represents only a 1 % increase in total anthropogenic NOx emissions.

The increases in agricultural emissions are most substantial over the Indian Subcontinent, followed by China, Egypt, southeast Asia and Brazil, and to a less degree in other Latin American countries, North America, West Asia and African savannah. The sharpest decline of agricultural emissions is observed in eastern Europe and Benelux, followed by milder declines across central Europe and Japan. According to the CEDS inventory, changes in agricultural emissions dominates the trend of total NH_3 emissions in all major regions except Africa, where large part of the NH_3 emissions trend is attributable to the waste management and the RCO (residential, commercial, other) sectors (Hoesly et al., 2018) (Figure S3). In contrast, the increase

https://doi.org/10.5194/acp-2021-132
Preprint. Discussion started: 23 March 2021


Atmospheric Chemistry and Physics Discussions

in agricultural emissions of NO_x does not contribute significantly to the global increase of total NO_x emissions over our period of concern.

We note that the hotspots of change in managed land cover and of change in agricultural emissions are not always overlapping. For example, agricultural emissions increase significantly over northern China and northern India, while the cropland coverage over those regions does not increase correspondingly over this same period. Similarly, agricultural emissions have declined over Kazakhstan, while the area of managed land has not decreased significantly. This highlights a degree of independence between land management and LULCC, with both being components of land change but having potentially distinct spatial patterns and impacts on air quality. This also highlights the importance of treating both in our chemical transport model simulations as they occur contemporaneously around the globe, and may have different impacts on air quality.

4 Impact of LULCC and agricultural emission changes on surface $PM_{2.5}$

Figure 5 shows the modeled impacts of LULCC, changes in agricultural emissions, and the combined effects of both, on annual mean surface $PM_{2.5}$ (under 2014 anthropogenic emissions). We have calculated the impacts of LULCC on $PM_{2.5}$ ("$\Delta PM_{2.5,\ LULCC}$" as the difference in $PM_{2.5}$ predicted by Simulation 2 and Simulation 1; the impacts of agricultural emission changes on $PM_{2.5}$ ("$\Delta PM_{2.5,\ agr\_emis}$") as the difference in $PM_{2.5}$ predicted by Simulation 3 and Simulation 2; and the impacts of these combined ("$\Delta PM_{2.5,\ LULCC+agr\_emis}$") as the difference in $PM_{2.5}$ predicted Simulation 3 and Simulation 1 (see Table 1).

The effect of LULCC on $PM_{2.5}$ (Fig. 5a) is mainly through perturbing BVOC emissions as they are a precursor to SOA. Over southern Amazonia and maritime southeast Asia, where isoprene emissions drop significantly due to deforestation, $PM_{2.5}$ is reduced by up to 0.7 μg m^{-3}. Land cover changes also lead to changes in the dry deposition velocity of some SNA precursor gases where stomatal uptakes is an important deposition pathway (e.g. NO_2 and SO_2, Fig. S4). Indeed, over northeastern India and eastern China, where our model suggests high levels of SNA aerosol precursors, contemporary LULCC enhances dry deposition of these constituents which reduces $PM_{2.5}$ overall by up to 0.3 μg m^{-3}, similar to the finding of Fu et al. (2016).

We find that the agricultural emissions generally have larger impact on annual mean surface $PM_{2.5}$ level (Fig. 5b) than LULCC. The largest increases in annual mean surface $PM_{2.5}$ due to changes in agricultural emissions over 1992 to 2014 occur across China (+0.7 μg m^{-3}) and India (+1.6 μg m^{-3}). Over some hot spots in the two countries (e.g. northwestern India and North China Plain), the local changes in $PM_{2.5}$ exceed >3.5 μg m^{-3}, supporting the previously emphasized importance of controlling NH_3 emissions on PM air quality of China (Fu et al., 2017), but potentially India as well. Some moderate increases (< 2 μg m^{-3} in most locations) in annual mean $PM_{2.5}$ concentrations are also observed in West Asia, Egypt, eastern US, Mexico, Peru and southeastern Brazil.

https://doi.org/10.5194/acp-2021-132
Preprint. Discussion started: 23 March 2021


Atmospheric Chemistry and Physics Discussions

The largest decreases in annual mean $PM_{2.5}$ due to changes in agricultural emissions are simulated in eastern Europe, particularly over Ukraine (-2.1 μg m^{-3}), Bulgaria (-1.5 μg m^{-3}) and Romania (-1.2 μg m^{-3}). In Russia, similarly large decreases are observed in the western and south Siberian part of the country. Despite comparable reductions in agricultural NH_3 emissions, decreases in $PM_{2.5}$ over the Benelux region are smaller because of weaker sensitivity of SNA aerosol to NH_3 emissions, which is consistent with the finding of Lee et al. (2015) and Pozzer et al. (2017). In general, reductions in annual mean $PM_{2.5}$ due to agricultural emission changes simulated over western Europe are weaker than over eastern Europe.

Figure 5c shows the combined effect of agricultural emissions and LULCC on annual mean surface $PM_{2.5}$, which we have already shown is mostly dominated by the effect of agricultural emissions. Nevertheless, we find that the effects of LULCC are able to partially offset the increase in $PM_{2.5}$ due to agricultural emissions changes over eastern China and northeastern India. These offsets are occurring in densely populated areas, so that the effects on population-weighted average $PM_{2.5}$ concentrations (see below), and therefore potentially exposure, may be noteworthy. This is discussed in further detail below.

We note that the difference between Figure S5a and Figure 5c illustrates how $\Delta PM_{2.5,\ LULCC+agr\_emis}$ is sensitive to the anthropogenic emissions background. We find that surface $PM_{2.5}$ over US, Europe and Former Soviet Union (FSU) are less sensitive to NH_3 emissions under 2014 anthropogenic emissions background, since both SO_2 and NO_x emissions in these regions have decreased significantly (> 42% for NO_x and > 58% for SO_2) over 1992 and 2014. The opposite is simulated in over China and India, where SO_2 and NO_x emissions have increased by >50%.

Table 3 summarizes the simulated effects of these land change phenomena on $PM_{2.5}$ air quality, and compares their magnitudes with the concomitant effects from direct anthropogenic emission changes ("$\Delta PM_{2.5,\ anth}$") over the same time period. We additionally compare area-averaged and population-weighted global and regional metrics. While the resolution of our simulations does not capture urban-scale gradients and non-linearities in urban chemistry, the use of population weighting allows us to explore whether signals of change in land cover or land management are concentrated over areas of high population, or whether they are primarily observed over less populated areas. The country definitions of each region in Table 2 are provided in Table S2 (and largely follow IMAGE 2.4 classifications).

Globally, our model results estimate that the global population-weighted change in $PM_{2.5}$ resulting from LULCC and agricultural emission changes (+0.70 μg m^{-3}) is on the order of ~10% of the change in $PM_{2.5}$ resulting from direct anthropogenic emissions (+7.99 μg m^{-3}) over 1992 to 2014. Regionally, the largest impact of land change ($\Delta PM_{2.5,\ LULCC+agr\_emis}$) on population-weighted annual mean surface $PM_{2.5}$ is simulated over CEU (-1.01 μg m^{-3}), FSU (-1.00 μg m^{-3}), SAs (+1.71 μg m^{-3}) and China (+1.45 μg m^{-3}). In most regions, the difference between population-weighted $\Delta PM_{2.5,\ agr\_emis}$ and $\Delta PM_{2.5,\ LULCC+agr\_emis}$ is very small (< ~0.05 μg m^{-3}) except in China (0.12 μg m^{-3}). Generally, the impacts of land change on population weighted $\Delta PM_{2.5}$ have the same sign as the impacts of direct anthropogenic emissions. The only exception to this occurs over

https://doi.org/10.5194/acp-2021-132
Preprint. Discussion started: 23 March 2021


Atmospheric Chemistry and Physics Discussions

North America (NAm) where anthropogenic NO_x and SO_2 emissions have declines, but agricultural emissions have increased. This suggests that the increase in agricultural emissions over NAm has partially canceled out the effects of other emission controls on $PM_{2.5}$, though this effect is small so far (~5%). In other regions, population-weighted $\Delta PM_{2.5,\ LULCC+agr\_emis}$ is generally on the order of 5% to 12% of changes due to direct anthropogenic emissions (e.g. in CEU and WEU). Notably, over FSU, the Middle East (ME), and central America (CAm), $\Delta PM_{2.5,\ LULCC+agr\_emis}$ are much more comparable to the effect of anthropogenic emission changes (24%, 42%, and 208% respectively).

Our result shows that the impact of LULCC and land management changes on $PM_{2.5}$ is mainly from the agricultural emission changes, while LULCC can result in additional impacts in regions with high SNA precursor emissions (e.g. India, China) through modulating dry deposition. The magnitude of population-weighted $\Delta PM_{2.5,\ LULCC+agr\_emis}$ suggests that land change may contribute significantly to regional and global changes in human $PM_{2.5}$ exposures and that the effects of these changes are not isolated to low population regions. Particularly, over the regions experiencing rapid change in land use intensity (e.g. FSU) or slow change in anthropogenic emissions (e.g. CAm, ME), the effects of land changes on particulate air pollution could be comparable (24% to 208%) to the effects of direct anthropogenic emission changes.

5 Impact on surface O_3

Figure 6 shows the modeled impacts of LULCC, changes in agricultural emissions, and the combined effects of both, on annual mean surface O_3 (under 2014 anthropogenic emissions). These changes are calculated identically as for $PM_{2.5}$ above: the impacts of LULCC on O_3 ("$\Delta O_{3,\ LULCC}$") is the difference in O_3 predicted by Simulation 2 and Simulation 1; the impacts of agricultural emission changes on O_3 ("$\Delta O_{3,\ agr\_emis}$") is the difference in $PM_{2.5}$ predicted by Simulation 3 and Simulation 2; and the impacts of these combined ("$\Delta O_{3,\ LULCC+agr\_emis}$") is the difference in $PM_{2.5}$ predicted Simulation 3 and Simulation 1 (see Table 1). We also use predictions of surface HNO_3/H_2O_2 ratios (Figure S6) as a proxy of VOC- vs NO_x- sensitive chemical O_3 production (Peng et al., 2006; Sillman, 1995) in our discussion of the results.

The modelled response of surface O_3 to LULCC ($\Delta O_{3,\ LULCC}$) (Fig. 6a) involves several distinct processes (dry deposition, soil NOx, and BVOC emissions). Over eastern US and central Mexico, the increase in dry deposition velocity (v_d) reduces annual mean surface ozone by up to 0.5 ppbv overall. In central Brazil, deforestation of tropical rainforests leads to significant reduction is isoprene emissions, reducing surface ozone by up to 0.8 ppbv in this NO_x-limited environment (Fig. S6). In contrast, modelled surface ozone increases by up to 1.2 ppbv over Bolivia and northern Argentina, where strong increases in LAI lead to largely increases v_d. The modelled reduction of surface ozone (up to 1 ppbv) over central African rainforests is also likely attributable to increased v_d as neither soil NOx nor isoprene emissions change much in the region. However, in other parts of sub-Saharan Africa, up to 0.6 ppbv of surface ozone increases are simulated, mainly because of the relatively large increase in soil NO emission. In southern China, up to 0.5 ppbv reduction in surface ozone is simulated, which is likely

https://doi.org/10.5194/acp-2021-132
Preprint. Discussion started: 23 March 2021


Atmospheric Chemistry and Physics Discussions

attributable to the increase in v_d, and slightly offset by the small increase in isoprene emission under this NO_x-saturated environment (Fig. S6).

Overall, the role of agricultural emission changes in fertilizer-associated NOx plays a minor role in surface O_3 changes (Fig. 6b). An exception to this is observed in the large increase in agricultural NO_x emissions in parts of Asia which reduce surface O_3 by up to 0.6 ppbv over NO_x-saturated northern India and eastern China, but increase surface O_3 in NO_x-limited Myanmar by similar magnitude. Slight increases in surface O_3 level due to increased agricultural NO_x emissions are also simulated over East Africa and southern Brazil. Whether the effect of agricultural emissions strengthens (e.g. eastern China and Sahel) or offset (e.g. over southern Brazil and northern India) is largely region-dependent. As shown in Fig. 6c, LULCC tend to dominate the impacts on surface O_3 over most regions in the world (unlike $PM_{2.5}$ where the effects of agricultural emission changes dominate).

Similar to $PM_{2.5}$, we find that the changes in anthropogenic emission background over 1992 to 2014 is strong enough to alter the sensitivity of O_3 to land change. As indicated by Fig. S6, Asia was less NO_x-saturated, while western Europe and coastal United States were more NO_x-saturated in 1992 than in 2014. For example, the increase in soil NO emission over India is more like to increase rather than decrease surface ozone concentration (fig. S7a), leading to different modelled effect on surface ozone.

Table 4 shows the change in area and population-weighted annual mean afternoon surface O_3 due to the effects of anthropogenic emissions ("$\Delta O_{3,\,anth}$", Fig. S7b), $\Delta O_{3,\,LULCC}$, $\Delta O_{3,\,agr\_emis}$ and $\Delta O_{3,\,LULCC+agr\_emis}$. In most regions, $\Delta O_{3,\,LULCC+agr\_emis}$ is positive. However, this is offset by the negative population-weighted average $\Delta O_{3,\,LULCC+agr\_emis}$ over the most populous regions (South Asia and China), resulting in very small globally averaged population-weighted $\Delta O_{3,\,LULCC+agr\_emis}$.

The magnitudes of population-weighted ΔO_3 (within ±0.5 ppbv) display less regional variability than that of $\Delta PM_{2.5}$. Over Eastern Africa (EAf), Western Africa (WAf) and Southern Africa (SAf), area-averaged $\Delta O_{3,\,agr\_emis+land\_cover}$ generally has similar magnitudes to population-weighted $\Delta O_{3,\,agr\_emis+land\_cover}$. In other regions, the differences between area and population-weighted $\Delta O_{3,\,LULCC+agr\_emis}$ are more substantial. The largest discrepancies between area and population-weighted $\Delta O_{3,\,LULCC+agr\_emis}$ is found over China, where increases in surface O_3 are predicted over less populated western China, while reductions in surface O_3 are simulated over more densely-populated eastern China. In South America (SAm), there are large sub-regional signals of $\Delta O_{3,\,LULCC+agr\_emis}$, but these the positive and negative largely offset each other, resulting both in small area-weighted and population-weighted $\Delta O_{3,\,LULCC+agr\_emis}$.

Over China, FSU, ME, WAf, EAf and SAf, the magnitudes of population-weighted $\Delta O_{3,\,LULCC+agr\_emis}$ are more than 20% of that of $\Delta O_{3,\,anth}$, implying that contemporary land system changes could be a regionally important component in contemporary

https://doi.org/10.5194/acp-2021-132
Preprint. Discussion started: 23 March 2021


Atmospheric Chemistry and Physics Discussions

trends of surface O_3. The effects of agricultural emission changes and LULCC can either noticeably enhance (e.g. over ME, JK, China) or offset (e.g. over, SAs) each other because of the dependence of $\Delta O_{3,\ agr\_emis+land\_cover}$ on regional NO_x-VOC chemistry and details of LULCC, indicating the complexity of diagnosing the effect of land change on surface O_3 at regional and global scale.

Our result suggests that contemporary agricultural emission changes and LULCC each have distinct effects on surface O_3, with LULCC generally stronger in magnitude. Both of the effects are dependent on local NO_x-VOC chemistry, as agricultural emission changes perturb NO_x emissions, while LULCC tends to affect BVOC emissions. In addition, LULCC is also able to affect surface O_3 (and other precursors) directly through dry deposition through LAI changes over our period of concern. These effects are found to affect O_3 pollution over densely populated regions (e.g. China) and could be comparable to the magnitudes of O_3 changes due to anthropogenic emissions over specific regions (e.g. FSU, EAf, WAf), indicating the importance of land change in studying long-term changes in surface O_3.

6 Impact on Nitrogen Deposition

Finally, we estimate the effect of these land changes on nitrogen deposition estimates. Figure 7 shows the global impact of LULCC and agricultural emission changes on total nitrogen deposition (ΔN_{dep}), and Table 5 summarizes the regional and global results. The largest increase and decrease in nitrogen deposition (N_{dep}) are simulated over SAs (+1.91 TgN yr^{-1}) and FSU (-1.28 TgN yr^{-1}), respectively. Notable increases in N_{dep} are also simulated over China (+1.55 TgN yr^{-1}), SAm (+1.24 TgN yr^{-1}), NAm (+0.66 TgN yr^{-1}), WAf (+0.39 TgN yr^{-1}) and EAf (+0.41 TgN yr^{-1}). Figure 7 also illustrates the simulated changes over 1992 to 2014 in area with nitrogen deposition (N_{dep}) exceeding 5 kgN ha^{-1} yr^{-1}, which is a proxy of possible exceedance of critical N_{dep} loads for terrestrial and fresh water (Moriarty, 1988).

Globally, there is a net increase in land area with N_{dep} > 5 kgN ha^{-1} yr^{-1} of 3.67×10^6 km^2. The increase is mostly simulated over the Americas, Africa, ME and China, which is partially offset the large decrease over FSU. Meanwhile, despite agricultural changes that lead to notable ΔN_{dep}, over most of Europe, eastern US, China, South Asia and Southeast Asia, nitrogen input from other sources are large enough that this signal alone does not lead substantial changes in N_{dep} exceedances of 5 kgN ha^{-1} yr^{-1}. However, over the periphery of North American Great Plain, southeastern part of South America, Nile River Delta, western China and African Savannah, agricultural changes are simulated to increase N_{dep} from below to above 5 kgN ha^{-1} yr^{-1}. This implies these natural ecosystems at the edge of these areas are at risk of nitrogen exceedances due to agricultural changes. In contrast, the substantial reduction of N_{dep} in southern Russia may have significantly reduce the risk of nitrogen exceedance of natural ecosystem from agricultural sources.

https://doi.org/10.5194/acp-2021-132
Preprint. Discussion started: 23 March 2021


Atmospheric Chemistry and Physics Discussions

7 Discussion and Conclusions

In this work, we have explored how changes in the global land system, through LULCC and agricultural emission changes, may have impacted contemporary global air quality over 1992 to 2014. We model the effects of contemporary LULCC and agricultural emission changes, individually then in combination, on surface O_3 and $PM_{2.5}$ using the GEOS-Chem CTM with a uniquely consistent framework that is able to integrate direct information from global emission inventories (CEDS) with updated land surface remote sensing products (ESACCI land cover and GLASS LAI) on surface O_3 and $PM_{2.5}$, allowing us to avoid invoking extra assumptions on land management practices (e.g. constant N_r input, emissions or emission factors over time) and biophysical properties of PFTs (e.g. constant PFT-specific LAI over time).

We find that changes in agricultural emissions are simulated to increase the annual mean surface $PM_{2.5}$ concentrations in China and India by up to 3.5 μg m^{-3} and to decrease in Europe by up to 3.5 μg m^{-3}. Our simulation suggests that though $\Delta PM_{2.5}$ is mainly attributable to changes in agricultural emissions in global scale, LULCC over northeastern India and eastern China can lead to enhanced dry deposition of certain $PM_{2.5}$ precursor gases (SO_2 and NO_2), thus partially offsetting (~10 %) the increase in $PM_{2.5}$ from agricultural regions. This implies a potentially important role of LULCC in determining SNA aerosol level over certain heavily polluted regions. Also, LULCC reduces BVOC emissions over Amazonia which lead to reductions in $PM_{2.5}$ by up to 0.7 μg m^{-3}. In a future with decreasing anthropogenic NO_x and SO_2 emissions, which could diminish the importance of agricultural emissions on $PM_{2.5}$ formation (Bauer et al., 2016), LULCC may become increasingly important in the overall effect of land change on $PM_{2.5}$. Noticeable changes (> 1 μg m^{-3}) population-weighted $\Delta PM_{2.5,\ LULCC+agr\_emis}$ are simulated over China (+1.45 μg m^{-3}), SAs (+1.71 μg m^{-3}), CEU (-1.00 μg m^{-3}) and FSU (-1.01 μg m^{-3}), indicating the potential impact of land change on long-term public health through modulating $PM_{2.5}$ level at regional scale. Our results suggest that contemporary (1996-2014) changes contribute to changes in $PM_{2.5}$ at regional and global scales that range from on the order of 5 to 10% of changes in $PM_{2.5}$ resulting from direct anthropogenic emissions over the same time period, and up to ~25% or more in FSU, ME and CAm specifically.

In contrast, the effect of LULCC is generally stronger than that of agricultural emission change in simulations of surface O_3. We find that the role of LULCC over 1992 to 2014 is regionally significant enough to induce changes in BVOC emissions and dry deposition which affect surface O_3, but that the overall effects largely offset each other on the global scale, leading to very small population-weighted $\Delta O_{3,\ LULCC+agr\_emis}$. Both the effects of agricultural emission changes and LULCC, through NO_x and BVOC emissions, are sensitive to regional ozone production regime. The increase in agricultural emissions reduces O_3 over NO_x-saturated China and SAs by up to 0.6 ppbv, while the reduction in BVOC emissions increases surface O_3 over VOC-limited Amazonia by up to 1.2 ppbv; enhancements of dry deposition reduce O_3 over Rio de la Plata Basin, eastern China, and eastern US by up to 1.2 ppbv. Overall, the largest population-weighted $\Delta O_{3,\ LULCC+agr\_emis}$ is simulated over WAf (+0.42 ppbv) and EAf (+0.47 ppbv). We find that the ratio between $\Delta O_{3,\ LULCC+agr\_emis}$ and $\Delta O_{3,\ anth}$ varies widely depending on region, with

https://doi.org/10.5194/acp-2021-132
Preprint. Discussion started: 23 March 2021


Atmospheric Chemistry and Physics Discussions

some having $\Delta O_{3,\ LULCC+agr\_emis}$ that are comparable (>20%) to $\Delta O_{3,\ anth}$. These results show the complexity and importance of land change on mediating long-term changes in surface O_3.

We also find that both the modelled $\Delta O_{3,\ LULCC+agr\_emis}$ and $\Delta PM_{2.5,\ LULCC+agr\_emis}$ are sensitive to the changes in anthropogenic emissions suggested by CEDS inventory over 1992 and 2014, as the changes in NO_x, SO_2 and VOC emissions are large enough to perturb atmospheric HNO_3 and H_2SO_4 production, and ozone production regime considerably in many regions (e.g. Asia and western Europe). This highlights the necessity of accurate and relevant emission inventories when evaluating the impacts of land change on air quality (e.g. Bauer et al., 2016).

The increased atmospheric reactive nitrogen (+7.20 Tg/yr) due to agricultural emissions is mostly found to deposit near to source region as the atmospheric lifetime of NH_3 is generally short, which implies the potential risk of excessive nitrogen input over the natural ecosystems near to the regions with increases in agricultural emissions.

Our work suggests that, at contemporary timescales (on the order of ~20 years), the effect of land change on air quality is contributes changes in air quality that can sometimes be important relative to changes induced by trends in direct anthropogenic emissions. We also find that agricultural emission changes have stronger effects on $PM_{2.5}$, while LULCC have stronger effects on O_3. This finding is comparable to that from Heald and Geddes (2016), which suggest a much more comparable changes in biogenic SOA (mostly induced by LULCC) and particulate nitrate (mostly induced by agricultural emission changes), and stronger surface ozone changes induced by land change over 1850 – 2000. This shows that both the magnitudes and relative contributions from different components of land change effects on air quality vary significantly as timescale of study, and its potential importance at longer timescales (e.g. multidecadal, centennial), despite the relative small signal that we obtain here.

We note several important limitations and opportunities for development. We were only able to evaluate our simulation extensively over Europe, North American and East Asia. In most other regions where such evaluation of SNA speciation is not feasible, the sensitivity of SNA formation to NH_3 emissions can be a major source of uncertainty. Given the changes in agricultural emissions have occurred in global scale, effort of monitoring SNA speciation outside North America and Europe (e.g. Weagle et al., 2018) is necessary for understanding the sensitivity of $PM_{2.5}$ to agricultural emissions in global extent. Better understanding of both the sources and sinks of HNO_3 (e.g. Heald et al., 2012; Holmes et al., 2019; Luo et al., 2019; Petetin et al., 2016) and nitrate partitioning (e.g. Vasilakos et al., 2018) are important for modelling SNA aerosol and its sensitivity to NH_3 emissions. NH_3 emissions estimates also carry large uncertainty (Crippa et al., 2018). The inherent inconsistency of long-term LAI time series derived from reflectance measured by different instruments (Jiang et al., 2017) and the use of static land cover maps also introduce uncertainty in the LAI retrieval (Fang et al., 2013) and the subsequently computed LAI changes and trends, and these have been shown to be important to changes in simulated O_3 in this study and elsewhere (Wong et al. 2019).

https://doi.org/10.5194/acp-2021-132
Preprint. Discussion started: 23 March 2021


Atmospheric Chemistry and Physics Discussions

Our study helps demonstrate the possible magnitudes and regional patterns of the impacts of contemporary LULCC and agricultural emission changes on $PM_{2.5}$ and O_3, and suggests that the combination of these factors should not be neglected in the study of regional and global air quality changes over multi-decade timescales. Our results confirm the potential importance of controlling agricultural emissions on improving $PM_{2.5}$ air quality, which could be practical as numerous feasible options exist for reducing agricultural emissions through optimizing livestock and crop production system (e.g. Ti et al., 2019). Furthermore, as increasing reactive nitrogen input and land use change are the two of the main strategies to meet the global demand for biomass-based products in the future (Foley et al., 2011), the distinct yet significant impacts of agricultural emissions and land use change on O_3, $PM_{2.5}$ and nitrogen deposition should be investigated as part of the overall environmental impacts of land system changes, especially when tradeoff between increasing land input and cropland expansion exists (e.g. Lotze-Campen et al., 2010; Mauser et al., 2015).

Code Availability

The source code of GEOS-Chem model is publically available (https://doi.org/10.5281/zenodo.3634864). The GEOS-Chem model output and other source code used in the project can be obtained by contacting the corresponding author (jgeddes@bu.edu).

Competing interests

The authors declare that they have no conflict of interest.

Author Contributions

AYHW and JAG developed the ideas for this study, formulated the methods, and designed the model experiments together. AYHW performed the chemical transport model simulations and data analysis, with input and feedback from JAG. Manuscript preparation was performed by AYHW, reviewed, edited, and approved by JAG.

Acknowledgement

This work was funded by an NSF CAREER grant (ATM-1750328) to project PI J.A. Geddes. We also thank the Global Modelling and Assimilation Office (GMAO) at NASA Goddard Flight Center for providing the MERRA-2 data, European Space Agency Climate Change Initiative (ESA CCI) for the land cover time series, Center for Global Change Data Processing and Analysis at Beijing Normal University (BNU) for GLASS LAI product.

https://doi.org/10.5194/acp-2021-132
Preprint. Discussion started: 23 March 2021

Atmospheric Chemistry and Physics Discussions

References

Amos, H. M., Jacob, D. J., Holmes, C. D., Fisher, J. A., Wang, Q., Yantosca, R. M., Corbitt, E. S., Galarneau, E., Rutter, A. P., Gustin, M. S., Steffen, A., Schauer, J. J., Graydon, J. A., St Louis, V. L., Talbot, R. W., Edgerton, E. S., Zhang, Y. and Sunderland, E. M.: Gas-particle partitioning of atmospheric Hg(II) and its effect on global mercury deposition, Atmos. Chem. Phys., 12(1), 591–603, doi:10.5194/acp-12-591-2012, 2012.

Ansari, A. S. and Pandis, S. N.: Response of inorganic PM to precursor concentrations, Environ. Sci. Technol., 32(18), 2706–2714, doi:10.1021/es971130j, 1998.

Bauer, S. E., Tsigaridis, K. and Miller, R.: Significant atmospheric aerosol pollution caused by world food cultivation, Geophys. Res. Lett., 43(10), 5394–5400, doi:10.1002/2016GL068354, 2016.

Bey, I., Jacob, D. J., Yantosca, R. M., Logan, J. A., Field, B. D., Fiore, A. M., Li, Q., Liu, H. Y., Mickley, L. J. and Schultz, M. G.: Global modeling of tropospheric chemistry with assimilated meteorology: Model description and evaluation, J. Geophys. Res. Atmos., 106(D19), 23073–23095, doi:10.1029/2001JD000807, 2001.

Bobbink, R., Hicks, K., Galloway, J., Spranger, T., Alkemade, R., Ashmore, M., Bustamante, M., Cinderby, S., Davidson, E., Dentener, F., Emmett, B., Erisman, J. W., Fenn, M., Gilliam, F., Nordin, A., Pardo, L. and De Vries, W.: Global assessment of nitrogen deposition effects on terrestrial plant diversity: A synthesis, Ecol. Appl., doi:10.1890/08-1140.1, 2010.

Bonan, G. B., Levis, S., Kergoat, L. and Oleson, K. W.: Landscapes as patches of plant functional types: An integrating concept for climate and ecosystem models, Global Biogeochem. Cycles, 16(2), 5-1-5–23, doi:10.1029/2000gb001360, 2002.

Claverie, M., Matthews, J. L., Vermote, E. F. and Justice, C. O.: A 30+ year AVHRR LAI and FAPAR climate data record: Algorithm description and validation, Remote Sens., 8(3), doi:10.3390/rs8030263, 2016.

Crippa, M., Guizzardi, D., Muntean, M., Schaaf, E., Dentener, F., Van Aardenne, J. A., Monni, S., Doering, U., Olivier, J. G. J., Pagliari, V. and Janssens-Maenhout, G.: Gridded emissions of air pollutants for the period 1970-2012 within EDGAR v4.3.2, Earth Syst. Sci. Data, 10(4), 1987–2013, doi:10.5194/essd-10-1987-2018, 2018.

Ellis, E. C.: Ecology in an anthropogenic biosphere, Ecol. Monogr., 85(3), 287–331, doi:10.1890/14-2274.1, 2015.

Ellis, E. C., Kaplan, J. O., Fuller, D. Q., Vavrus, S., Goldewijk, K. K. and Verburg, P. H.: Used planet: A global history, Proc. Natl. Acad. Sci. U. S. A., 110(20), 7978–7985, doi:10.1073/pnas.1217241110, 2013.

ESA. Land Cover CCI Product User Guide Version 2. Tech. Rep. (2017). Available at: maps.elie.ucl.ac.be/CCI/viewer/download/ESACCI-LC-Ph2-PUGv2_2.0.pdf

Fang, H., Li, W. and Myneni, R. B.: The Impact of Potential Land Cover Misclassification on MODIS Leaf Area Index (LAI) Estimation: A Statistical Perspective, Remote Sens., 5(2), 830–844, doi:10.3390/rs5020830, 2013.

Fenn, M. E., Baron, J. S., Allen, E. B., Rueth, H. M., Nydick, K. R., Geiser, L., Bowman, W. D., Sickman, J. O., Meixner, T., Johnson, D. W. and Neitlich, P.: Ecological effects of nitrogen deposition in the western United States, Bioscience, doi:10.1641/0006-3568(2003)053[0404:EEONDI]2.0.CO;2, 2003.

Foley, J. A., Ramankutty, N., Brauman, K. A., Cassidy, E. S., Gerber, J. S., Johnston, M., Mueller, N. D., O'Connell, C., Ray, D. K., West, P. C., Balzer, C., Bennett, E. M., Carpenter, S. R., Hill, J., Monfreda, C., Polasky, S., Rockström, J., Sheehan, J., Siebert, S., Tilman, D. and Zaks, D. P. M.: Solutions for a cultivated planet, Nature, 478(7369), 337–342, doi:10.1038/nature10452, 2011.

Fountoukis, C. and Nenes, A.: ISORROPIAII: A computationally efficient thermodynamic equilibrium model for K+-Ca2+-

https://doi.org/10.5194/acp-2021-132
Preprint. Discussion started: 23 March 2021

Atmospheric Chemistry and Physics Discussions

Mg2+-NH4+-Na+-SO42--NO3--Cl--H2O aerosols, Atmos. Chem. Phys., 7(17), 4639–4659, doi:10.5194/acp-7-4639-2007, 2007.

Fu, X., Wang, S., Xing, J., Zhang, X., Wang, T. and Hao, J.: Increasing Ammonia Concentrations Reduce the Effectiveness of Particle Pollution Control Achieved via SO2 and NOX Emissions Reduction in East China, Environ. Sci. Technol. Lett., 4(6), 221–227, doi:10.1021/acs.estlett.7b00143, 2017.

Fu, Y. and Tai, A. P. K.: Impact of climate and land cover changes on tropospheric ozone air quality and public health in East Asia between 1980 and 2010, Atmos. Chem. Phys., 15(17), 10093–10106, doi:10.5194/acp-15-10093-2015, 2015.

Fu, Y., Tai, A. P. K. and Liao, H.: Impacts of historical climate and land cover changes on fine particulate matter (PM2.5) air quality in East Asia between 1980 and 2010, Atmos. Chem. Phys., 16(16), 10369–10383, doi:10.5194/acp-16-10369-2016, 2016.

Galloway, J. N., Townsend, A. R., Erisman, J. W., Bekunda, M., Cai, Z., Freney, J. R., Martinelli, L. A., Seitzinger, S. P. and Sutton, M. A.: Transformation of the nitrogen cycle: Recent trends, questions, and potential solutions, Science (80-.)., doi:10.1126/science.1136674, 2008.

Ganzeveld, L., Bouwman, L., Stehfest, E., van Vuuren, D. P., Eickhout, B. and Lelieveld, J.: Impact of future land use and land cover changes on atmospheric chemistry-climate interactions, J. Geophys. Res., 115(D23), D23301, doi:10.1029/2010JD014041, 2010.

Geddes, J. A. and Martin, R. V.: Global deposition of total reactive nitrogen oxides from 1996 to 2014 constrained with satellite observations of NO2 columns, Atmos. Chem. Phys., 17(16), 10071–10091, doi:10.5194/acp-17-10071-2017, 2017.

Geddes, J. A., Heald, C. L., Silva, S. J. and Martin, R. V.: Land cover change impacts on atmospheric chemistry: Simulating projected large-scale tree mortality in the United States, Atmos. Chem. Phys. Discuss., 15(20), 29303–29345, doi:10.5194/acpd-15-29303-2015, 2015.

Geddes, J. A., Heald, C. L., Silva, S. J. and Martin, R. V.: Land cover change impacts on atmospheric chemistry: Simulating projected large-scale tree mortality in the United States, Atmos. Chem. Phys., 16(4), 2323–2340, doi:10.5194/acp-16-2323-2016, 2016.

Gelaro, R., McCarty, W., Suárez, M. J., Todling, R., Molod, A., Takacs, L., Randles, C. A., Darmenov, A., Bosilovich, M. G., Reichle, R., Wargan, K., Coy, L., Cullather, R., Draper, C., Akella, S., Buchard, V., Conaty, A., da Silva, A. M., Gu, W., Kim, G. K., Koster, R., Lucchesi, R., Merkova, D., Nielsen, J. E., Partyka, G., Pawson, S., Putman, W., Rienecker, M., Schubert, S. D., Sienkiewicz, M. and Zhao, B.: The modern-era retrospective analysis for research and applications, version 2 (MERRA-2), J. Clim., 30(14), 5419–5454, doi:10.1175/JCLI-D-16-0758.1, 2017.

Giannadaki, D., Giannakis, E., Pozzer, A. and Lelieveld, J.: Estimating health and economic benefits of reductions in air pollution from agriculture, Sci. Total Environ., 622–623, 1304–1316, doi:10.1016/j.scitotenv.2017.12.064, 2018.

Goldewijk, K. K., Beusen, A., Doelman, J. and Stehfest, E.: Anthropogenic land use estimates for the Holocene - HYDE 3.2, Earth Syst. Sci. Data, 9(2), 927–953, doi:10.5194/essd-9-927-2017, 2017.

Guenther, A. B., Jiang, X., Heald, C. L., Sakulyanontvittaya, T., Duhl, T., Emmons, L. K. and Wang, X.: The model of emissions of gases and aerosols from nature version 2.1 (MEGAN2.1): An extended and updated framework for modeling biogenic emissions, Geosci. Model Dev., 5(6), 1471–1492, doi:10.5194/gmd-5-1471-2012, 2012.

Hansen, M. C., Potapov, P. V., Moore, R., Hancher, M., Turubanova, S. A., Tyukavina, A., Thau, D., Stehman, S. V., Goetz, S. J., Loveland, T. R., Kommareddy, A., Egorov, A., Chini, L., Justice, C. O. and Townshend, J. R. G.: High-resolution global maps of 21st-century forest cover change, Science (80-.)., doi:10.1126/science.1244693, 2013.

https://doi.org/10.5194/acp-2021-132
Preprint. Discussion started: 23 March 2021

Atmospheric Chemistry and Physics Discussions

Hardacre, C. J., Palmer, P. I., Baumanns, K., Rounsevell, M. and Murray-Rust, D.: Probabilistic estimation of future emissions of isoprene and surface oxidant chemistry associated with land-use change in response to growing food needs, Atmos. Chem. Phys., 13(11), 5451–5472, doi:10.5194/acp-13-5451-2013, 2013.

Heald, C. L. and Geddes, J. A.: The impact of historical land use change from 1850 to 2000 on secondary particulate matter and ozone, Atmos. Chem. Phys., 16(23), 14997–15010, doi:10.5194/acp-16-14997-2016, 2016.

Heald, C. L. and Spracklen, D. V.: Land Use Change Impacts on Air Quality and Climate, Chem. Rev., 115(10), 4476–4496, doi:10.1021/cr500446g, 2015.

Heald, C. L., Henze, D. K., Horowitz, L. W., Feddema, J., Lamarque, J. F., Guenther, A., Hess, P. G., Vitt, F., Seinfeld, J. H., Godstein, A. H. and Fung, I.: Predicted change in global secondary organic aerosol concentrations in response to future climate, emissions, and land use change, J. Geophys. Res. Atmos., 113(5), doi:10.1029/2007JD009092, 2008.

Heald, C. L., Collett, J. L., Lee, T., Benedict, K. B., Schwandner, F. M., Li, Y., Clarisse, L., Hurtmans, D. R., Van Damme, M., Clerbaux, C., Coheur, P. F., Philip, S., Martin, R. V. and Pye, H. O. T.: Atmospheric ammonia and particulate inorganic nitrogen over the United States, Atmos. Chem. Phys., 12(21), 10295–10312, doi:10.5194/acp-12-10295-2012, 2012.

Hoesly, R. M., Smith, S. J., Feng, L., Klimont, Z., Janssens-Maenhout, G., Pitkanen, T., Seibert, J. J., Vu, L., Andres, R. J., Bolt, R. M., Bond, T. C., Dawidowski, L., Kholod, N., Kurokawa, J. I., Li, M., Liu, L., Lu, Z., Moura, M. C. P., O'Rourke, P. R. and Zhang, Q.: Historical (1750-2014) anthropogenic emissions of reactive gases and aerosols from the Community Emissions Data System (CEDS), Geosci. Model Dev., doi:10.5194/gmd-11-369-2018, 2018.

Hollaway, M. J., Arnold, S. R., Collins, W. J., Folberth, G. and Rap, A.: Sensitivity of midnineteenth century tropospheric ozone to atmospheric chemistry-vegetation interactions, J. Geophys. Res. Atmos., 122(4), 2452–2473, doi:10.1002/2016JD025462, 2017.

Holmes, C. D., Bertram, T. H., Confer, K. L., Graham, K. A., Ronan, A. C., Wirks, C. K. and Shah, V.: The Role of Clouds in the Tropospheric NOx Cycle: A New Modeling Approach for Cloud Chemistry and Its Global Implications, Geophys. Res. Lett., 46(9), 4980–4990, doi:10.1029/2019GL081990, 2019.

Hudman, R. C., Moore, N. E., Mebust, A. K., Martin, R. V., Russell, A. R., Valin, L. C. and Cohen, R. C.: Steps towards a mechanistic model of global soil nitric oxide emissions: Implementation and space based-constraints, Atmos. Chem. Phys., 12(16), 7779–7795, doi:10.5194/acp-12-7779-2012, 2012.

Jiang, C., Ryu, Y., Fang, H., Myneni, R., Claverie, M. and Zhu, Z.: Inconsistencies of interannual variability and trends in long-term satellite leaf area index products, Glob. Chang. Biol., 23(10), 4133–4146, doi:10.1111/gcb.13787, 2017.

Kaplan, J. O., Krumhardt, K. M., Ellis, E. C., Ruddiman, W. F., Lemmen, C. and Goldewijk, K. K.: Holocene carbon emissions as a result of anthropogenic land cover change, Holocene, 21(5), 775–791, doi:10.1177/0959683610386983, 2011.

Keenan, R. J., Reams, G. A., Achard, F., de Freitas, J. V., Grainger, A. and Lindquist, E.: Dynamics of global forest area: Results from the FAO Global Forest Resources Assessment 2015, For. Ecol. Manage., 352, 9–20, doi:10.1016/j.foreco.2015.06.014, 2015.

Kim, P. S., Jacob, D. J., Fisher, J. A., Travis, K., Yu, K., Zhu, L., Yantosca, R. M., Sulprizio, M. P., Jimenez, J. L., Campuzano-Jost, P., Froyd, K. D., Liao, J., Hair, J. W., Fenn, M. A., Butler, C. F., Wagner, N. L., Gordon, T. D., Welti, A., Wennberg, P. O., Crounse, J. D., St. Clair, J. M., Teng, A. P., Millet, D. B., Schwarz, J. P., Markovic, M. Z. and Perring, A. E.: Sources, seasonality, and trends of Southeast US aerosol: An integrated analysis of surface, aircraft, and satellite observations with the GEOS-Chem chemical transport model, Atmos. Chem. Phys. Discuss., 15(13), 17651–17709, doi:10.5194/acpd-15-17651-2015, 2015.

https://doi.org/10.5194/acp-2021-132
Preprint. Discussion started: 23 March 2021

Atmospheric Chemistry and Physics Discussions

Lai, L., Huang, X., Yang, H., Chuai, X., Zhang, M., Zhong, T., Chen, Z., Chen, Y., Wang, X. and Thompson, J. R.: Carbon emissions from land-use change and management in China between 1990 and 2010, Sci. Adv., 2(11), doi:10.1126/sciadv.1601063, 2016.

Lawrence, P. J. and Chase, T. N.: Representing a new MODIS consistent land surface in the Community Land Model (CLM 3.0), J. Geophys. Res. Biogeosciences, 112(1), G01023, doi:10.1029/2006JG000168, 2007.

Lee, C. J., Martin, R. V., Henze, D. K., Brauer, M., Cohen, A. and Donkelaar, A. Van: Response of global particulate-matter-related mortality to changes in local precursor emissions, Environ. Sci. Technol., doi:10.1021/acs.est.5b00873, 2015.

Lelieveld, J., Evans, J. S., Fnais, M., Giannadaki, D. and Pozzer, A.: The contribution of outdoor air pollution sources to premature mortality on a global scale, Nature, 525(7569), 367–371, doi:10.1038/nature15371, 2015.

Li, W., Macbean, N., Ciais, P., Defourny, P., Lamarche, C., Bontemps, S., Houghton, R. A. and Peng, S.: Gross and net land cover changes in the main plant functional types derived from the annual ESA CCI land cover maps (1992-2015), Earth Syst. Sci. Data, 10(1), 219–234, doi:10.5194/essd-10-219-2018, 2018.

Liu, H., Jacob, D. J., Bey, I. and Yantosca, R. M.: Constraints from 210Pb and 7Be on wet deposition and transport in a global three-dimensional chemical tracer model driven by assimilated meteorological fields, J. Geophys. Res. Atmos., 106(D11), 12109–12128, doi:10.1029/2000JD900839, 2001.

Lotze-Campen, H., Popp, A., Beringer, T., Müller, C., Bondeau, A., Rost, S. and Lucht, W.: Scenarios of global bioenergy production: The trade-offs between agricultural expansion, intensification and trade, Ecol. Modell., 221(18), 2188–2196, doi:10.1016/j.ecolmodel.2009.10.002, 2010.

Luo, G., Yu, F. and Schwab, J.: Revised treatment of wet scavenging processes dramatically improves GEOS-Chem 12.0.0 simulations of surface nitric acid, nitrate, and ammonium over the United States, Geosci. Model Dev., doi:10.5194/gmd-12-3439-2019, 2019.

Mao, J., Paulot, F., Jacob, D. J., Cohen, R. C., Crounse, J. D., Wennberg, P. O., Keller, C. A., Hudman, R. C., Barkley, M. P. and Horowitz, L. W.: Ozone and organic nitrates over the eastern United States: Sensitivity to isoprene chemistry, J. Geophys. Res. Atmos., 118(19), 11256–11268, doi:10.1002/jgrd.50817, 2013.

Mauser, W., Klepper, G., Zabel, F., Delzeit, R., Hank, T., Putzenlechner, B. and Calzadilla, A.: Global biomass production potentials exceed expected future demand without the need for cropland expansion, Nat. Commun., 6, doi:10.1038/ncomms9946, 2015.

Moriarty, F.: Air quality guidelines for Europe, Environ. Pollut., 55(1), 77, doi:10.1016/0269-7491(88)90163-7, 1988.

Murray, L. T., Jacob, D. J., Logan, J. A., Hudman, R. C. and Koshak, W. J.: Optimized regional and interannual variability of lightning in a global chemical transport model constrained by LIS/OTD satellite data, J. Geophys. Res. Atmos., 117(20), doi:10.1029/2012JD017934, 2012.

Paulot, F. and Jacob, D. J.: Hidden cost of U.S. agricultural exports: Particulate matter from ammonia emissions, Environ. Sci. Technol., 48(2), 903–908, doi:10.1021/es4034793, 2014.

Payne, R. J., Dise, N. B., Field, C. D., Dore, A. J., Caporn, S. J. M. and Stevens, C. J.: Nitrogen deposition and plant biodiversity: past, present, and future, Front. Ecol. Environ., doi:10.1002/fee.1528, 2017.

Peng, Y. P., Chen, K. S., Lai, C. H., Lu, P. J. and Kao, J. H.: Concentrations of H2O2 and HNO3 and O3-VOC-NOx sensitivity in ambient air in southern Taiwan, Atmos. Environ., doi:10.1016/j.atmosenv.2006.05.079, 2006.

Petetin, H., Sciare, J., Bressi, M., Gros, V. rie, Rosso, A., Sanchez, O., Sarda-Est ve, R., Petit, J. E. and Beekmann, M.: Assessing the ammonium nitrate formation regime in the Paris megacity and its representation in the CHIMERE model, Atmos. Chem. Phys., 16(16), 10419–10440, doi:10.5194/acp-16-10419-2016, 2016.

Pinder, R. W., Adams, P. J. and Pandis, S. N.: Ammonia emission controls as a cost-effective strategy for reducing atmospheric particulate matter in the Eastern United States, Environ. Sci. Technol., 41(2), 380–386, doi:10.1021/es060379a, 2007.

Potapov, P. V., Turubanova, S. A., Tyukavina, A., Krylov, A. M., McCarty, J. L., Radeloff, V. C. and Hansen, M. C.: Eastern Europe's forest cover dynamics from 1985 to 2012 quantified from the full Landsat archive, Remote Sens. Environ., 159, 28–43, doi:10.1016/j.rse.2014.11.027, 2015.

Pozzer, A., Tsimpidi, A. P., Karydis, V. A., De Meij, A. and Lelieveld, J.: Impact of agricultural emission reductions on fine-particulate matter and public health, Atmos. Chem. Phys., 17(20), 12813–12826, doi:10.5194/acp-17-12813-2017, 2017.

Reick, C. H., Raddatz, T., Brovkin, V. and Gayler, V.: Representation of natural and anthropogenic land cover change in MPI-ESM, J. Adv. Model. Earth Syst., 5(3), 459–482, doi:10.1002/jame.20022, 2013.

Sillman, S.: The use of NOy, H2O2, and HNO3 as indicators for ozone-NOx- hydrocarbon sensitivity in urban locations, J. Geophys. Res., doi:10.1029/94JD02953, 1995.

Silva, S. J., Heald, C. L., Geddes, J. A., Austin, K. G., Kasibhatla, P. S. and Marlier, M. E.: Impacts of current and projected oil palm plantation expansion on air quality over Southeast Asia, Atmos. Chem. Phys., 16(16), 10621–10635, doi:10.5194/acp-16-10621-2016, 2016.

Sobota, D. J., Compton, J. E., McCrackin, M. L. and Singh, S.: Cost of reactive nitrogen release from human activities to the environment in the United States, Environ. Res. Lett., doi:10.1088/1748-9326/10/2/025006, 2015.

Sofen, E. D., Bowdalo, D., Evans, M. J., Apadula, F., Bonasoni, P., Cupeiro, M., Ellul, R., Galbally, I. E., Girgzdiene, R., Luppo, S., Mimouni, M., Nahas, A. C., Saliba, M. and Tørseth, K.: Gridded global surface ozone metrics for atmospheric chemistry model evaluation, Earth Syst. Sci. Data, doi:10.5194/essd-8-41-2016, 2016.

Song-Miao Fan, Wofsy, S. C., Bakwin, P. S., Jacob, D. J. and Fitzjarrald, D. R.: Atmosphere-biosphere exchange of CO2 and O3 in the central Amazon forest, J. Geophys. Res., 95(D10), doi:10.1029/jd095id10p16851, 1990.

Squire, O. J., Archibald, A. T., Abraham, N. L., Beerling, D. J., Hewitt, C. N., Lathière, J., Pike, R. C., Telford, P. J. and Pyle, J. A.: Influence of future climate and cropland expansion on isoprene emissions and tropospheric ozone, Atmos. Chem. Phys., 14(2), 1011–1024, doi:10.5194/acp-14-1011-2014, 2014.

Steinkamp, J. and Lawrence, M. G.: Improvement and evaluation of simulated global biogenic soil NO emissions in an AC-GCM, Atmos. Chem. Phys., 11(12), 6063–6082, doi:10.5194/acp-11-6063-2011, 2011.

Sustainable United Nations: Buildings and Climate Change: Summary for Decision Makers, Build. Clim. Chang. Summ. Decis., 15(3), 1–62, doi:10.1127/0941-2948/2006/0130, 2009.

Tai, A. P. K., Mickley, L. J., Heald, C. L. and Wu, S.: Effect of CO2 inhibition on biogenic isoprene emission: Implications for air quality under 2000 to 2050 changes in climate, vegetation, and land use, Geophys. Res. Lett., 40(13), 3479–3483, doi:10.1002/grl.50650, 2013.

Ti, C., Xia, L., Chang, S. X. and Yan, X.: Potential for mitigating global agricultural ammonia emission: A meta-analysis, Environ. Pollut., doi:10.1016/j.envpol.2018.10.124, 2019.

Vasilakos, P., Russell, A., Weber, R. and Nenes, A.: Understanding nitrate formation in a world with less sulfate, Atmos.

https://doi.org/10.5194/acp-2021-132
Preprint. Discussion started: 23 March 2021

Atmospheric Chemistry and Physics Discussions

Chem. Phys., 18(17), 12765–12775, doi:10.5194/acp-18-12765-2018, 2018.

WallisDeVries, M. F. and Bobbink, R.: Nitrogen deposition impacts on biodiversity in terrestrial ecosystems: Mechanisms and perspectives for restoration, Biol. Conserv., doi:10.1016/j.biocon.2017.01.017, 2017.

Wang, Q., Jacob, D. J., Fisher, J. A., Mao, J., Leibensperger, E. M., Carouge, C. C., Le Sager, P., Kondo, Y., Jimenez, J. L., Cubison, M. J. and Doherty, S. J.: Sources of carbonaceous aerosols and deposited black carbon in the Arctic in winter-spring: Implications for radiative forcing, Atmos. Chem. Phys., doi:10.5194/acp-11-12453-2011, 2011.

Wang, Q., Jacob, D. J., Spackman, J. R., Perring, A. E., Schwarz, J. P., Moteki, N., Marais, E. A., Ge, C., Wang, J. and Barrett, S. R. H.: Global budget and radiative forcing of black carbon aerosol: Constraints from pole-to-pole (HIPPO) observations across the Pacific, J. Geophys. Res., doi:10.1002/2013JD020824, 2014.

Wang, Y., Jacob, D. J. and Logan, J. A.: Global simulation of tropospheric O 3-NO x-hydrocarbon chemistry - 1. Model formulation, J. Geophys. Res. D Atmos., 103(3339), 10713–10725, doi:10.1029/98jd00158, 1998.

Weagle, C. L., Snider, G., Li, C., Van Donkelaar, A., Philip, S., Bissonnette, P., Burke, J., Jackson, J., Latimer, R., Stone, E., Abboud, I., Akoshile, C., Anh, N. X., Brook, J. R., Cohen, A., Dong, J., Gibson, M. D., Griffith, D., He, K. B., Holben, B. N., Kahn, R., Keller, C. A., Kim, J. S., Lagrosas, N., Lestari, P., Khian, Y. L., Liu, Y., Marais, E. A., Martins, J. V., Misra, A., Muliane, U., Pratiwi, R., Quel, E. J., Salam, A., Segev, L., Tripathi, S. N., Wang, C., Zhang, Q., Brauer, M., Rudich, Y. and Martin, R. V.: Global Sources of Fine Particulate Matter: Interpretation of PM 2.5 Chemical Composition Observed by SPARTAN using a Global Chemical Transport Model, Environ. Sci. Technol., 52(20), 11670–11681, doi:10.1021/acs.est.8b01658, 2018.

Van Der Werf, G. R., Randerson, J. T., Giglio, L., Van Leeuwen, T. T., Chen, Y., Rogers, B. M., Mu, M., Van Marle, M. J. E., Morton, D. C., Collatz, G. J., Yokelson, R. J. and Kasibhatla, P. S.: Global fire emissions estimates during 1997-2016, Earth Syst. Sci. Data, 9(2), 697–720, doi:10.5194/essd-9-697-2017, 2017.

Wesely, M. L.: Parameterization of surface resistances to gaseous dry deposition in regional-scale numerical models, Atmos. Environ., 41(SUPPL.), 52–63, doi:10.1016/j.atmosenv.2007.10.058, 1989.

Wu, S., Mickley, L. J., Kaplan, J. O. and Jacob, D. J.: Impacts of changes in land use and land cover on atmospheric chemistry and air quality over the 21st century, Atmos. Chem. Phys., 12(3), 1597–1609, doi:10.5194/acp-12-1597-2012, 2012a.

Wu, S., Mickley, L. J., Kaplan, J. O. and Jacob, D. J.: Impacts of changes in land use and land cover on atmospheric chemistry and air quality over the 21st century, Atmos. Chem. Phys., 12(3), 1597–1609, doi:10.5194/acp-12-1597-2012, 2012b.

Xiao, Z., Liang, S., Wang, J., Xiang, Y., Zhao, X. and Song, J.: Long-Time-Series Global Land Surface Satellite Leaf Area Index Product Derived from MODIS and AVHRR Surface Reflectance, IEEE Trans. Geosci. Remote Sens., 54(9), 5301–5318, doi:10.1109/TGRS.2016.2560522, 2016.

Xu, R., Tian, H., Pan, S., Prior, S. A., Feng, Y., Batchelor, W. D., Chen, J. and Yang, J.: Global ammonia emissions from synthetic nitrogen fertilizer applications in agricultural systems: Empirical and process-based estimates and uncertainty, Glob. Chang. Biol., 25(1), 314–326, doi:10.1111/gcb.14499, 2019.

Zhang, L., Gong, S., Padro, J. and Barrie, L.: A size-segregated particle dry deposition scheme for an atmospheric aerosol module, Atmos. Environ., 35(3), 549–560, doi:10.1016/S1352-2310(00)00326-5, 2001.

Zhu, Z., Bi, J., Pan, Y., Ganguly, S., Anav, A., Xu, L., Samanta, A., Piao, S., Nemani, R. R. and Myneni, R. B.: Global data sets of vegetation leaf area index (LAI)3g and fraction of photosynthetically active radiation (FPAR)3g derived from global inventory modeling and mapping studies (GIMMS) normalized difference vegetation index (NDVI3G) for the period 1981 to 2, Remote Sens., 5(2), 927–948, doi:10.3390/rs5020927, 2013.

https://doi.org/10.5194/acp-2021-132
Preprint. Discussion started: 23 March 2021

710 Zhu, Z., Piao, S., Myneni, R. B., Huang, M., Zeng, Z., Canadell, J. G., Ciais, P., Sitch, S., Friedlingstein, P., Arneth, A., Cao, C., Cheng, L., Kato, E., Koven, C., Li, Y., Lian, X., Liu, Y., Liu, R., Mao, J., Pan, Y., Peng, S., Peuelas, J., Poulter, B., Pugh, T. A. M., Stocker, B. D., Viovy, N., Wang, X., Wang, Y., Xiao, Z., Yang, H., Zaehle, S. and Zeng, N.: Greening of the Earth and its drivers, Nat. Clim. Chang., 6(8), 791–795, doi:10.1038/nclimate3004, 2016.

715

720

725

730

735

740

https://doi.org/10.5194/acp-2021-132
Preprint. Discussion started: 23 March 2021

Atmospheric Chemistry and Physics Discussions

	1	2	3	4	5
Agricultural emissions	1992	1992	1992	2014	2014
Land cover	1992	1992	2014	2014	2014
Anthropogenic emissions	1992	2014	2014	2014	1992

Table 1. Model configurations. The numbers in the top row are referred to in the main text.

Land cover	**Coverage at 1992 (km^2)**	**Coverage at 2015 (km^2)**	**Change (km^2)**
Needleleaf forest	1.115×10^7	1.106×10^7	-8.892×10^4 (-0.8%)
Broadleaf forest	2.146×10^7	2.092×10^7	-5.409×10^5 (-2.5%)
Natural grass and shrub	3.769×10^7	3.768×10^7	-2.067×10^4 (-0.1%)
Managed grass	2.127×10^7	2.199×10^7	$+7.157 \times 10^5$ (+3.4%)
Built-up area	2.603×10^5	5.966×10^5	$+2.948 \times 10^5$ (+113%)

Table 2. Global LULCC summarized by the changes in coverage of different land types (2014 – 1992) from ESACCI land cover product

https://doi.org/10.5194/acp-2021-132
Preprint. Discussion started: 23 March 2021

Atmospheric Chemistry and Physics Discussions

Region†	$\Delta PM_{2.5(anth)}$	$\Delta PM_{2.5(LULCC)}$	$\Delta PM_{2.5(agr\_emis)}$	$\Delta PM_{2.5(LULCC+agr\_emis)}$
FSU	-1.33 (-4.18)	+0.00 (+0.01)	-0.42 (-1.02)	-0.41 (-1.00)
CEU	-7.36 (-8.14)	-0.01 (-0.01)	-0.90 (-0.99)	-0.90 (-0.99)
WEU	-4.01 (-8.40)	-0.01 (-0.01)	-0.19 (-0.41)	-0.20 (-0.42)
China	+8.32 (+19.6)	-0.03 (-0.11)	+0.72 (+1.57)	+0.70 (+1.45)
SAs	+11.6 (+17.6)	-0.02 (-0.05)	+1.21 (+1.77)	+1.19 (+1.71)
ME	+1.16 (+1.06)	+0.01 (+0.01)	+0.29 (+0.43)	+0.30 (+0.44)
NAm	-1.58 (-5.44)	-0.00 (-0.01)	+0.07 (+0.28)	+0.07 (+0.27)
CAm	-0.37 (-0.12)	-0.01 (-0.01)	+0.11 (+0.25)	+0.11 (+0.25)
Global	+0.22 (+7.99)	-0.01 (-0.04)	+0.01 (+0.74)	+0.00 (+0.70)

Table 3. Changes in area averaged, and population-weighted (in parentheses), annual mean surface $PM_{2.5}$ concentrations (in μg m^{-3}) due to anthropogenic emissions alone ($\Delta PM_{2.5(anth)}$), LULCC ($\Delta PM_{2.5(LULCC)}$), agricultural emissions ($\Delta PM_{2.5(agr\_emis)}$), and the combined effects of LULCC and agricultural emission ($\Delta PM_{2.5(LULCC+agr\_emis)}$) together. Results only from regions with $\Delta PM_{2.5(LULCC)}$, $\Delta PM_{2.5(agr\_emis)}$ or $\Delta PM_{2.5(LULCC+agr\_emis)}$ > 0.2 μg m^{-3} are shown. †The definitions and abbreviations of all regions can be found in Table S2.

Region†	$\Delta O_{3(anth)}$	$\Delta O_{3(LULCC)}$	$\Delta O_{3(agr\_emis)}$	$\Delta O_{3(LULCC+agr\_emis)}$
FSU	-0.06 (+0.41)	+0.08 (+0.25)	+0.02 (+0.00)	+0.10 (+0.25)
China	+1.41 (-1.13)	+0.20 (-0.10)	+0.00 (-0.14)	+0.21 (-0.24)
SAs	+3.80 (+3.41)	+0.35 (+0.25)	-0.12 (-0.25)	+0.22 (-0.01)
ME	+1.98 (+0.74)	+0.35 (+0.28)	-0.05 (-0.06)	+0.31 (+0.23)
WAf	+1.22 (+1.99)	+0.36 (+0.33)	+0.05 (+0.08)	+0.41 (+0.42)
SAf	+0.95 (+1.10)	+0.30 (+0.25)	+0.02 (+0.02)	+0.32 (+0.27)
EAf	+1.53 (+1.92)	+0.31 (+0.29)	+0.10 (+0.18)	+0.41 (+0.47)
Global	+0.79 (+1.70)	+0.09 (+0.08)	+0.02 (-0.06)	+0.11 (+0.02)

Table 4. Changes in area averaged and population-weighted (in parentheses) annual mean surface O_3 concentrations (in ppbv) due to anthropogenic emissions alone ($\Delta PM_{2.5(anth)}$), LULCC ($\Delta PM_{2.5(LULCC)}$), agricultural emissions ($\Delta PM_{2.5(agr\_emis)}$), and the combined effects of LULCC and agricultural emission ($\Delta PM_{2.5(LULCC+agr\_emis)}$) together. Results only from regions with population-weighted average $\Delta O_{3(LULCC)}$, $\Delta O_{3(agr\_emis)}$ or $\Delta O_{3(LULCC+agr\_emis)}$ > 0.2 ppb are shown. †The definitions and abbreviations of all regions can be found in Table S2.

https://doi.org/10.5194/acp-2021-132
Preprint. Discussion started: 23 March 2021

Atmospheric Chemistry and Physics Discussions

Region†	ΔN_{dep} (TgN yr^{-1})	$\Delta Area_{crit}$ (1000 km^2)
FSU	-1.28	-1064
China	+1.55	+502
SAs	+1.91	0
ME	+0.29	+494
SEA	+0.61	+244
NAm	+0.66	+788
SAm	+1.24	+1467
WAf	+0.39	+487
SAf	+0.15	+363
EAf	+0.41	+364
Global	+7.20	+3673

Table 5. Changes in total nitrogen deposition (ΔN_{dep}) and land area that has nitrogen deposition > 5 kgN ha^{-1} yr^{-1} ($\Delta Area_{crit}$), which is a proxy of potential risk of critical nitrogen deposition load exceedance. Only regions with significant ΔN_{dep} (> 0.25 TgN yr^{-1}) or $\Delta Area_{crit}$ (> 10^5 km^2) are shown.

†The definitions and abbreviations of all regions can be found in Table S2.

https://doi.org/10.5194/acp-2021-132
Preprint. Discussion started: 23 March 2021

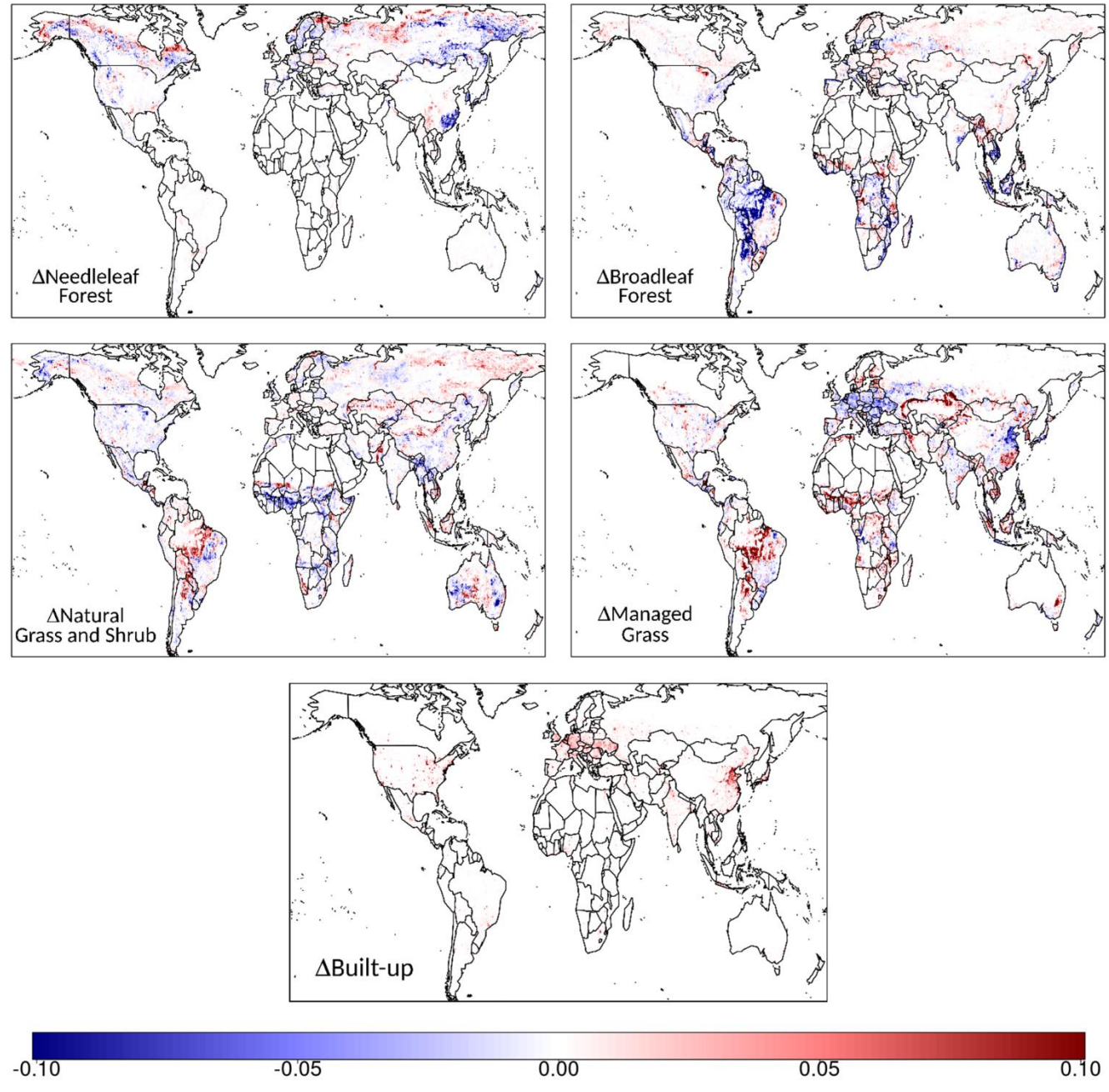

Figure 1. Global spatial patterns of 2014-1992 LULCC characterized by the changes in coverages (unitless) of major land cover types derived from the ESA CCI land cover product.

https://doi.org/10.5194/acp-2021-132
Preprint. Discussion started: 23 March 2021

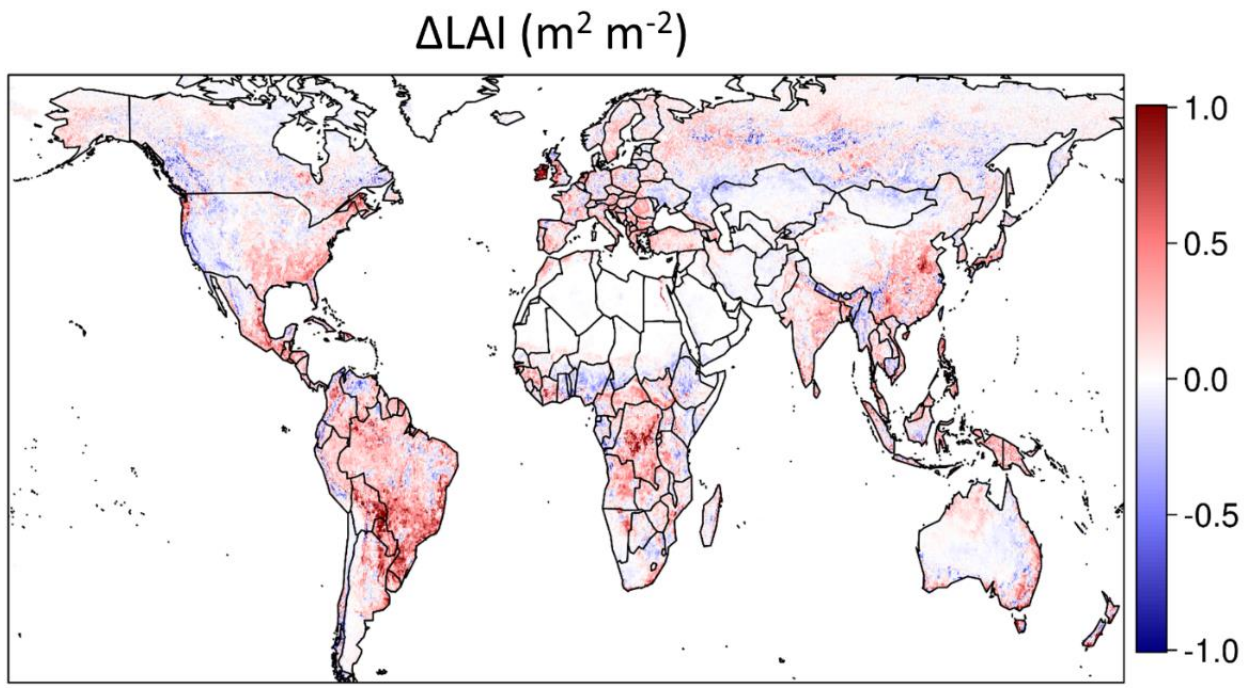

Figure 2. GLASS-derived changes in 3-year mean annual LAI (2012 to 2014 average minus 1991 to 1993 average).

https://doi.org/10.5194/acp-2021-132
Preprint. Discussion started: 23 March 2021

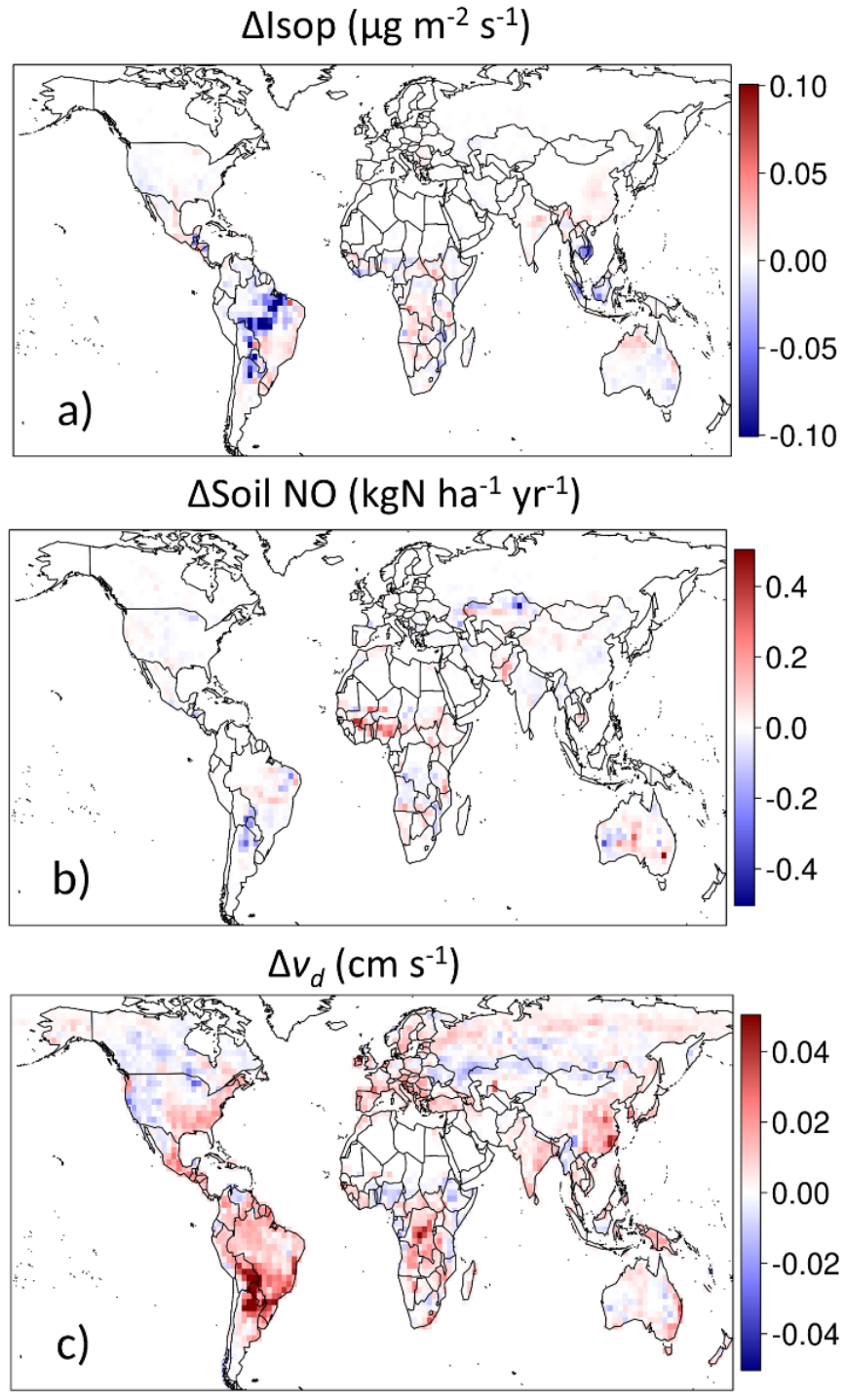

Figure 3. Changes in annual mean a) isoprene emission (ΔIsop), b) soil NO emission (ΔSoil NO), and c) O_3 dry deposition velocity (Δv_d), due to LULCC over 1992 and 2014.

https://doi.org/10.5194/acp-2021-132
Preprint. Discussion started: 23 March 2021

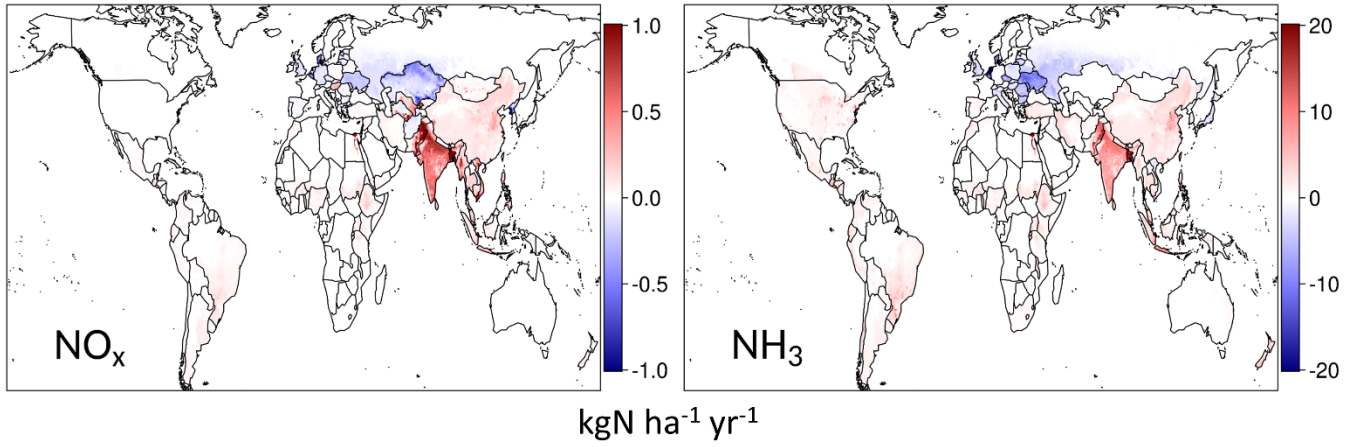

Figure 4. Changes in agricultural NH_3 and NO_x emissions (2014 – 1992) as implemented by CEDS.

https://doi.org/10.5194/acp-2021-132
Preprint. Discussion started: 23 March 2021

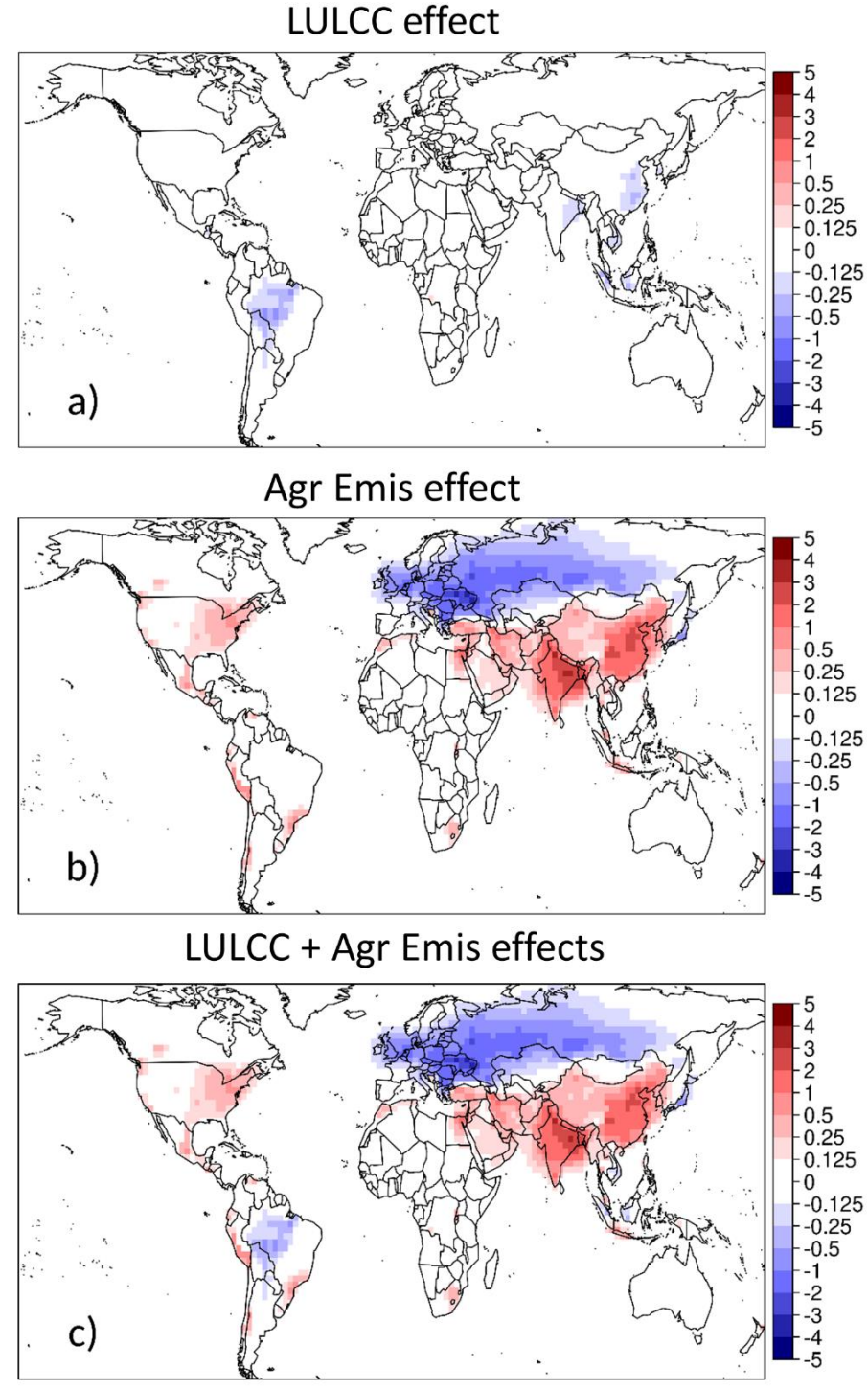

Figure 5. Simulated changes in annual mean surface $PM_{2.5}$ due to (a) LULCC, (b) agricultural emission changes, and (c) the combined effects of agricultural emissions and LULCC.

https://doi.org/10.5194/acp-2021-132
Preprint. Discussion started: 23 March 2021

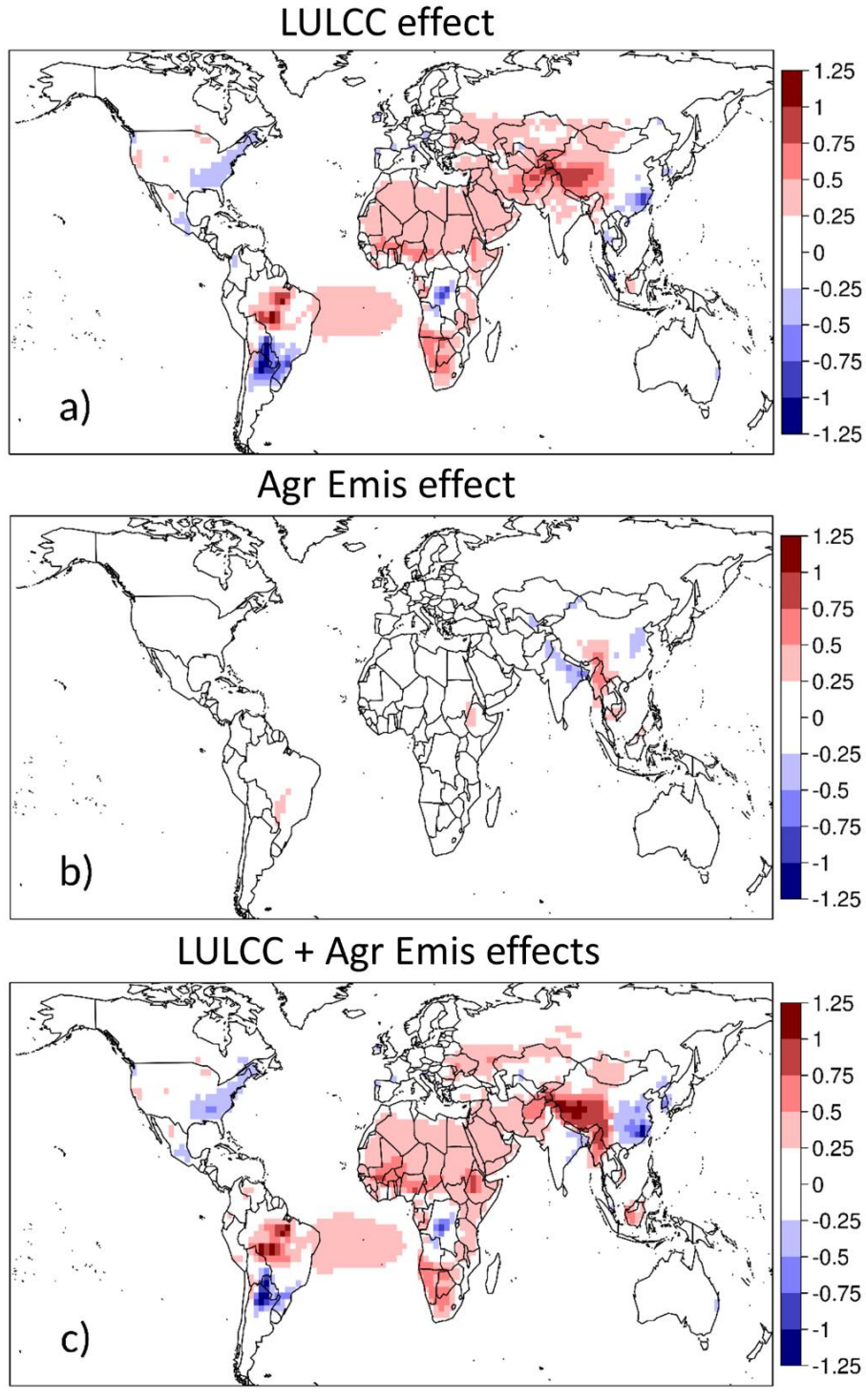

Figure 6. Simulated changes in annual mean surface O_3 due to (a) LULCC, (b) agricultural emission changes, and (c) the combined effects of agricultural emissions and LULCC.

https://doi.org/10.5194/acp-2021-132
Preprint. Discussion started: 23 March 2021

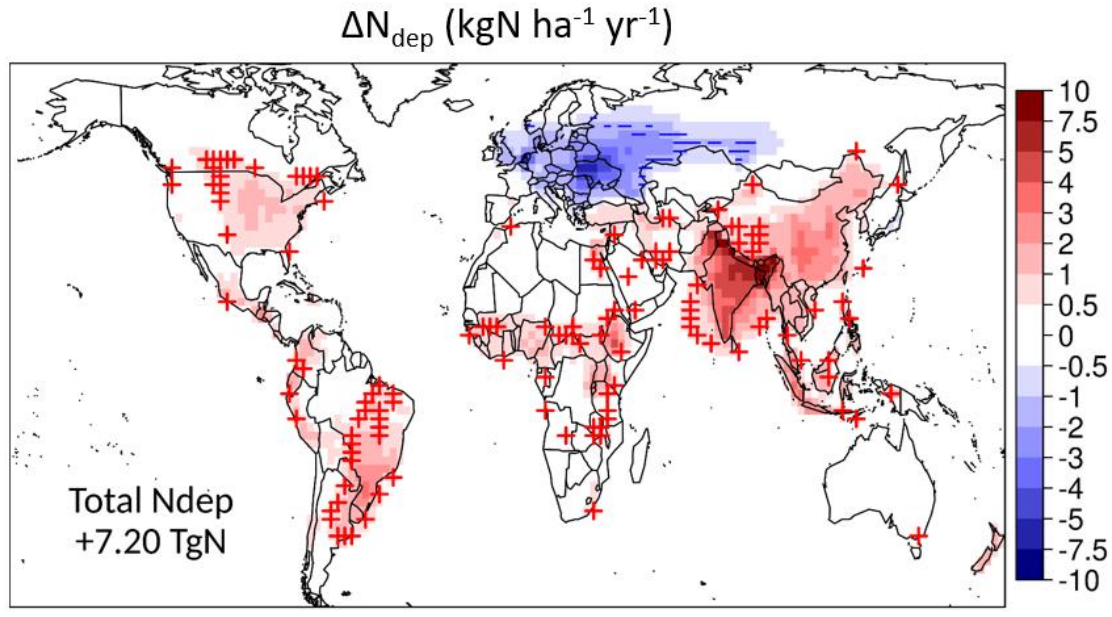

Figure 7. Changes in total nitrogen deposition (ΔN_{dep}) due to changes (1992-2014) in agricultural emissions and land cover. Red plus signs (+) mark new gridcells where total nitrogen deposition exceeds 5 kg N ha-1 yr-1, while blue minus signs (-) denote the gridcells where total nitrogen deposition decreases to below 5 kgN ha^{-1} yr^{-1}.